

Fall 2009

# Optimal synthesis of planar adjustable mechanisms

Chong Peng

*New Jersey Institute of Technology*

Follow this and additional works at: <https://digitalcommons.njit.edu/dissertations>



Part of the [Mechanical Engineering Commons](#)

---

## Recommended Citation

Peng, Chong, "Optimal synthesis of planar adjustable mechanisms" (2009). *Dissertations*. 196.  
<https://digitalcommons.njit.edu/dissertations/196>

This Dissertation is brought to you for free and open access by the Theses and Dissertations at Digital Commons @ NJIT. It has been accepted for inclusion in Dissertations by an authorized administrator of Digital Commons @ NJIT. For more information, please contact [digitalcommons@njit.edu](mailto:digitalcommons@njit.edu).

## **Copyright Warning & Restrictions**

**The copyright law of the United States (Title 17, United States Code) governs the making of photocopies or other reproductions of copyrighted material.**

**Under certain conditions specified in the law, libraries and archives are authorized to furnish a photocopy or other reproduction. One of these specified conditions is that the photocopy or reproduction is not to be “used for any purpose other than private study, scholarship, or research.” If a user makes a request for, or later uses, a photocopy or reproduction for purposes in excess of “fair use” that user may be liable for copyright infringement,**

**This institution reserves the right to refuse to accept a copying order if, in its judgment, fulfillment of the order would involve violation of copyright law.**

**Please Note: The author retains the copyright while the New Jersey Institute of Technology reserves the right to distribute this thesis or dissertation**

**Printing note: If you do not wish to print this page, then select “Pages from: first page # to: last page #” on the print dialog screen**

The Van Houten library has removed some of the personal information and all signatures from the approval page and biographical sketches of theses and dissertations in order to protect the identity of NJIT graduates and faculty.

## ABSTRACT

### OPTIMAL SYNTHESIS OF PLANAR ADJUSTABLE MECHANISMS

by  
Chong Peng

Adjustable mechanisms provide degrees of flexibility while retaining desirable features of one degree of freedom close-loop mechanisms, such as simplicity, stability, and high speed capabilities. By adjusting linkage parameters, additional phases of motions can be achieved using the same hardware. However, an adjustment to the mechanism adds only one or two additional design positions and divides desired positions into “phases”, each of which contains only a few positions usually insufficient for industrial applications.

In order to extend the design position limitation of adjustable mechanisms, an optimal synthesis method based on link length structural error is developed and applied to kinematic synthesis of adjustable planar mechanisms in this research. Designed with this method, adjustable mechanisms can achieve phases of many design positions with a minimized error. The conveniently-calculated link length structural error effectively reflects the overall difference between generated and desired motions without directly comparing them; and its compact fourth-order polynomial form facilitates the gradient-based optimization process.

Link length structural error based optimal synthesis methods are developed for adjustable planar four-bar mechanisms for three typical synthesis tasks. For multi-phase approximate motion generation, standard optimization model is established based on adjustable optimal dyads considering all types of adjustments. For multi-phase continuous path generation, a proper driving dyad is firstly found by an optimization procedure using the full rotation requirement. The driven dyad is then found using the

optimization technique for motion generation after calculating all coupler angles. For multi-phase function generation, the coupler length is chosen to carry the structural error and adjustments to the coupler and the side-link lengths are considered.

Numerical synthesis examples have demonstrated that the developed method is effective and efficient for multi-phase motion, path, and function generation of planar four-bar linkages with a large number of specified positions in each phase.

# **OPTIMAL SYNTHESIS OF PLANAR ADJUSTABLE MECHANISMS**

by  
**Chong Peng**

**A Dissertation  
Submitted to the Faculty of  
New Jersey Institute of Technology  
in Partial Fulfillment of the Requirements for the Degree of  
Doctor of Philosophy in Mechanical Engineering**

**Department of Mechanical and Industrial Engineering**

**January 2010**

Copyright © 2010 by Chong Peng

ALL RIGHTS RESERVED

APPROVAL PAGE

OPTIMAL SYNTHESIS OF PLANAR ADJUSTABLE MECHANISMS

Chong Peng

Dr. Rajpal S. Sodhi, Dissertation Advisor  
Professor of Mechanical Engineering, NJIT

12/15/09  
Date

Dr. Bernard Koplik, Committee Member  
Professor of Mechanical Engineering, NJIT

12/15/09  
Date

Dr. Chao Zhu, Committee Member  
Professor of Mechanical Engineering, NJIT

12/15/09  
Date

Dr. Zhiming Ji, Committee Member  
Associate Professor of Mechanical Engineering, NJIT

12/14/2009  
Date

Dr. Kevin Russell, Committee Member  
Senior Engineer, Armament Engineering and Technology Center, Picatinny, NJ

12/14/09  
Date



## BIOGRAPHICAL SKETCH

**Author:** Chong Peng  
**Degree:** Doctor of Philosophy  
**Date:** January 2010

### **Undergraduate and Graduate Education:**

- Doctor of Philosophy in Mechanical Engineering,  
New Jersey Institute of Technology, Newark, NJ, 2010
- Master of Science in Mechanics,  
University of Science and Technology of China, Hefei, Anhui, P. R. China, 2004
- Bachelor of Engineering in Mechanical Engineering,  
University of Science and Technology of China, Hefei, Anhui, P. R. China, 2001

**Major:** Mechanical Engineering

### **Presentations and Publications:**

Chong Peng, Rajpal S. Sodhi, Optimal synthesis of adjustable mechanisms generating multi-phase approximate paths, submitted to Mechanism and Machine Theory, under second review.

Chong Peng, Peiqiang Zhang, An optical-fiber interferometer for the dynamic characterization of microstructures, International Journal of Information Acquisition 1 (2004) 129-134.

To my beloved parents, wife, and baby.

## **ACKNOWLEDGMENT**

I would like to gratefully and sincerely thank Dr. Rajpal S. Sodhi for his guidance, understanding, patience, and most importantly, his friendship during my doctoral study at New Jersey Institute of Technology.

I would like to thank Dr. Bernard Kopik, Dr. Chao Zhu, Dr. Zhiming Ji, and Dr. Kevin Russell for participating in my committee. Special thanks are also given to Dr. Kevin Russell for his advice and help during this research.

I would like to thank my parents, my wife, my baby, and all other family members for their support and encouragement throughout my study.

## TABLE OF CONTENTS

Chapter	Page
1 INTRODUCTION.....	1
1.1 Kinematic Synthesis .....	1
1.2 Adjustable Mechanisms .....	2
1.2.1 Introduction.....	2
1.2.2 Existing Synthesis Methods.....	4
1.3 Optimal Synthesis.....	11
1.3.1 Procedure of Optimal Synthesis.....	12
1.3.2 Structural Error.....	12
1.3.3 Optimal Synthesis Methods.....	15
1.4 Research Objectives.....	21
2 OPTIMAL SYNTHESIS BASED ON LINK LENGTH STRUCTURAL ERROR.....	23
2.1 Link Length Structural Error.....	23
2.1.1 Formulation.....	23
2.1.2 Validation.....	27
2.2 Optimization Model.....	31
2.3 Optimization Algorithm.....	32
2.4 Synthesis Examples.....	35
2.4.1 Optimal Motion Generation.....	36
2.4.2 Continuous Path Generation.....	39

**TABLE OF CONTENTS**  
**(Continued)**

<b>Chapter</b>	<b>Page</b>
2.5 Conclusion.....	41
<b>3 OPTIMAL MULTI-PHASE MOTION GENERATION .....</b>	<b>43</b>
3.1 Multi-phase Approximate Motion Generation.....	43
3.2 Adjustable Dyad for Optimal Motion Generation.....	44
3.2.1 Three Types of Adjustments.....	44
3.2.2 Combination of Adjustments.....	48
3.2.3 More Phases.....	49
3.3 Optimal Synthesis of Adjustable Four-bar Motion Generation Linkages.....	50
3.3.1 The Two Dyads Combined.....	50
3.3.2 Constraints.....	52
3.4 Continuously Adjustable Mechanisms.....	53
3.5 Synthesis Example.....	54
3.6 Conclusion.....	57
<b>4 OPTIMAL MULTI-PHASE PATH GENERATION .....</b>	<b>58</b>
4.1 Introduction.....	58
4.2 Multiple Continuous Path Generation Problem.....	59
4.3 Optimal Multiple Path Generation: Adjustable Driven Dyad.....	60
4.3.1 Synthesis of the Driving Dyad.....	61
4.3.2 Determining Coupler Angles.....	64
4.3.3 Optimal Synthesis of the Adjustable Driven Dyad.....	66

**TABLE OF CONTENTS**  
**(Continued)**

<b>Chapter</b>	<b>Page</b>
4.3.4 Continuous Adjustment.....	67
4.4 Optimal Multiple Path Generation: Adjustable Driving Dyad.....	68
4.5 Synthesis Example.....	69
4.6 Conclusion.....	72
5 OPTIMAL MULTI-PHASE FUNCTION GENERATION.....	74
5.1 Introduction to Optimal Function Generation.....	74
5.2 Optimal Function Generation Based on Coupler Link Length Structural Error.....	76
5.2.1 Linear Spacing.....	76
5.2.2 Coupler Link Length Structural Error.....	77
5.2.3 Validation.....	78
5.2.4 Constraints.....	80
5.3 Multiple Approximate Function Generation.....	81
5.3.1 Adjustable Coupler Link Length.....	82
5.3.2 Adjustable Side Link Length.....	83
5.4 Numerical Examples.....	84
5.5 Conclusion.....	88
6 CONCLUSION.....	89
REFERENCES.....	92

## LIST OF TABLES

<b>Table</b>	<b>Page</b>
1.1 Maximum Number of Design Positions of a Four-bar Linkage.....	4
2.1 Desired and Generated Positions.....	37
2.2 First 5 Local Minimums.....	38
2.3 Coordinates of Resulted Four-bar Linkage Joints in Their First position.....	38
2.4 Desired and Generated Path Points.....	40
2.5 Synthesized Four-bar Path Generation Linkage.....	40
3.1 Desired Two Phases of Rigid Body Positions.....	55
3.2 Optimized Adjustable Linkage.....	55
3.3 Generated Motions.....	56
4.1 Desired Path Points.....	70
4.2 Joint Positions of the Synthesized Adjustable Linkage.....	71
5.1 Desired Input and Output Angles.....	85
5.2 Optimized Adjustable Function Generating Linkage.....	85

## LIST OF FIGURES

Figure	Page
1.1 An adjustable motion generation linkage.....	3
1.2 A motion generation dyad.....	6
1.3 The desired and generated paths.....	13
1.4 Optimal path generation of a four-bar linkage.....	14
1.5 A deformable linkage model.....	16
1.6 A four-bar crank-rocker path generation linkage.....	17
1.7 The driving dyad of the four-bar path generator.....	19
2.1 The link length structural error.....	24
2.2 A four-bar linkage with a driven-side link length error.....	28
2.3 A four-bar linkage with a driving crank length error.....	30
2.4 Diagram of Sequential Quadratic Programming algorithm.....	35
2.5 The four-bar linkage and the desired and generated motions.....	38
2.6 The optimized linkage with the desired and the generated paths.....	41
3.1 An optimal dyad with adjustable link length for motion generation.....	45
3.2 Adjustable moving pivots for both dyads.....	51
3.3 A grab feeding material to two conveyers.....	54
3.4 The optimized adjustable linkage.....	57
4.1 The desired paths and a sample adjustable linkage.....	60
4.2 $R_{\max}$ and $R_{\min}$ of the driving dyad.....	62
4.3 The crank and coupler angles.....	65



**LIST OF FIGURES**  
**(Continued)**

<b>Figure</b>	<b>Page</b>
4.4 Desired paths.....	69
4.5 The synthesized linkage with the generated and the desired paths.....	72
5.1 A four-bar function generator.....	75
5.2 The coupler link length structural error.....	78
5.3 A four-bar function generator with coupler link length error.....	79
5.4 The four-bar function generator with adjustable coupler link length.....	82
5.5 The optimized adjustable function generator.....	86
5.6 The desired and generated functions: (a) $y=\sin x$ ; (b) $y=x^{1.5}$ .....	87

## CHAPTER 1

### INTRODUCTION

#### 1.1 Kinematic Synthesis

*Kinematic Synthesis* is the process of determining the geometry of a mechanism to produce a desired motion. The areas of kinematic synthesis may be grouped into two categories [1]. *Type synthesis* determines the type of mechanism, number of links, degrees of freedom, configuration of linkage, etc. On the other hand, *dimensional synthesis* seeks to determine the significant dimensions and the starting position of a mechanism of preconceived type for a specified task and prescribed performance. This research deals with dimensional synthesis of planar mechanisms.

There are three customary tasks for kinematic synthesis: motion, path, and function generation. *Motion generation* in mechanism synthesis requires a rigid body to be guided through a series of prescribed positions; therefore it is also called *rigid body guidance*. In *path generation* problems, a single point on the coupler is to follow a nominated curve. There are two sub-types of path generation. One is to specify only a small number of precision points on the path, and the trajectory between any two points is not required strictly, thus called point-to-point path generation. The other is to specify the whole path or many points on the path, while not requires them to be passed through exactly, and is called continuous path generation. *Function generation* is to coordinate the angles of the two cranks. The name “function generation” originated in the days in which mechanical analog computers were used to perform complex mathematical calculations.

## 1.2 Adjustable Mechanisms

### 1.2.1 Introduction

Conventional linkage mechanisms provide high speed capability at a low cost, but fail to provide the flexibility required in many industrial applications. On the other hand, for most manufacturing automation applications, expensive multi-axis robots are employed for simple repetitive operations that require only limited flexibility. In order to provide a middle ground between conventional mechanism-based automation and overly flexible robots, adjustable mechanisms were introduced.

Adjustable mechanisms add more functions to the same mechanism hardware by simply adjusting some of the linkage parameters. They offer more flexibility required in industrial applications while retaining desirable features of one degree of freedom close-loop mechanisms, such as simplicity, stability, and high speed, high load, and high precision capabilities, thus increasingly addressed interests of mechanism designers since 1960's.

The capability of generating multi-phase motions is the most desirable feature of adjustable mechanisms because industrial applications usually prefer the same linkage hardware to fulfill different tasks. For example, a manipulator may need to switch its destination between two workbenches, as shown in Figure 1.1. Other than a three degree-of-freedom "robot", which needs tremendous efforts on planning paths of its manipulator and managing its complicated actuators and sensors, a simple one degree-of-freedom adjustable motion generator can fulfill the task. In this case, a simple adjustment to the driven side-link length makes the linkage capable of switching its destination between the two workbenches as desired.

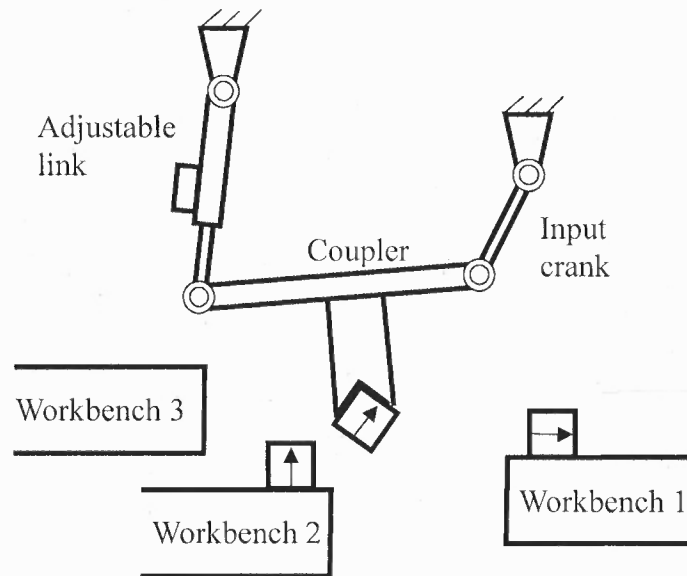


**Figure 1.1** An adjustable motion generation linkage.

Adjustable mechanisms also extend the maximum number of design positions a non-adjustable mechanism can achieve. Researchers have found that a linkage can only achieve a limited number of prescribed precision positions. For example, a four-bar linkage in general can guide its coupler through up to five given rigid body positions in motion generation, move its coupler point through up to nine points, or generate at most five input-output angle pairs. This is due to the mechanism's limited number of independent design variables compared to the required number of constraining equations. Table 1.1 lists the maximum number of design positions of a four-bar linkage in motion, path, and function generation. Additional design positions can be achieved by adjustable mechanisms because the adjustments add additional design variables. One adjustment usually adds one or two scalar unknowns to the linkage and thus adds one or two design positions.

**Table 1.1** Maximum Number of Design Positions of a Four-bar Linkage

Task	No. of scalar variables	No. of scalar equations	Maximum of n
Motion generation (dyad form)	$n+3^{\dagger}$	$2(n-1)$	5
Path generation (loop equations)	$n+7$	$2(n-1)$	9
Function generation (loop equations)	$n+5$	$2(n-1)$	$7^{\dagger\dagger}$

<sup>†</sup>  $n$  is the number of design positions. <sup>††</sup> Two of these variables are associated with the scaling and rotation of the linkage. If the scaled or rotated linkage is considered the same as the original one, the two variables are not free choices; the maximum of  $n$  is then 5.

There are three basic types of adjustments: the adjustment to the fixed pivot, moving pivot, or the link length. Combinations of these basic adjustments are also feasible.

As a compromise between traditional one-DOF linkages and modern multi-DOF robots, adjustable mechanisms add limited degrees of flexibility and cost more for the adjustments compared to the non-adjustable linkages, but cost less and achieve less flexibility than multi-axis robots. Thus to use or not to use adjustable mechanisms depends on the nature of the task: if the level of flexibility required by the task can not be provided by conventional non-adjustable mechanisms, one should first check adjustable mechanisms; and robots are the last ones to consider. Typical tasks suitable for adjustable mechanisms are those that need repetitive operation but sometimes also need to switch between several different predetermined modes. Arbitrary changes of motions can not be achieved by adjustable mechanisms and multi-DOF systems have to be employed.

## 1.2.2 Existing Synthesis Methods

### *a. Multi-phase motion generation*

Various synthesis techniques have been developed for adjustable mechanisms generating multiple motions.

Early effort to synthesize adjustable mechanisms was made by Bonnell [2] with a graphical approach. Though not as accurate and general as numerical methods, graphical synthesis techniques played an important role in mechanism synthesis and are still used today, usually for a quick check of initial guesses for optimization processes.

As computers greatly enhanced mechanism designers' capability of solving complicated nonlinear equation systems, analytical complex number methods prevailed. These methods use complex numbers to model mechanism links and apply vector algorithms to linkage movements to form loop equations, which are solved for linkage parameters.

For motion generation, loop equations usually take a dyad form; thus synthesis methods for adjustable motion generation mechanisms usually utilize a motion generating dyad model with adjustment(s) and combine two or more adjustable dyads to form a linkage, and two or more adjustments are generally required.

Synthesis methods based on adjustable dyads were reported by many researchers. Chuenchom and Kota [7, 8] solved vector equations of an adjustable dyad for two-phase five-position problem and found equations for the circle point curves and the center point curves with respect to varying ratio of side-link length adjustment. Two adjustable dyads were assembled to form an adjustable linkage. The synthesis procedure also worked with adjustments of coupler link length and position of fixed pivot.

Wilhelm [6] examined three types of adjustments: the side-link fixed pivot adjustment, the side-link length adjustment, and the combined adjustment of the two, and developed techniques for two-phase motion generation problems of four-bar linkages with two adjustable side-links.

Methods not using adjustable dyads were also reported. Ahmad and Waldron [3, 4] adjusted the driven crank fixed pivot position of a four-bar motion generating linkage and enumerated all the possible combination of maximum motion specifications for the two phases, which led to four classes of motion generation problems. Up to five prescribed positions in two phases can be generated by this method. Their loop equations consisted of both dyads.

Instead of complex-number modeling, Wang and Sodhi [9, 10] used the constant length condition for the crank to formulate scalar synthesis equations for adjustable motion generation mechanisms. As the dyad shown in Figure 1.2, for a two-phase adjustable moving pivot problem with three positions in each phase, the moving pivot  $C$  has a local coordinates  $(p_1, q_1)$  in phase one and is moved to  $(p_2, q_2)$  in phase two, with respect to frame  $X'AY'$  fixed to the coupler link. The link  $SC$  has to maintain its length for both phases, which leads to

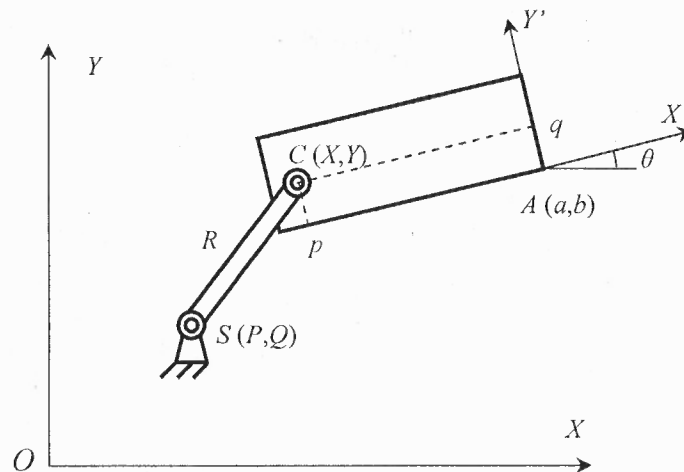


**Figure 1.2** A motion generation dyad.

$$(X_i - P)^2 + (Y_i - Q)^2 = R^2, i = 1, 2, 3, 4, 5, 6 \quad (1.1)$$

where  $R$  is the length of link  $SC$  and

$$\begin{aligned} X_i &= a_i + p_1 \cos \theta_i - q_1 \sin \theta_i, Y_i = b_i + p_1 \sin \theta_i + q_1 \cos \theta_i; i = 1, 2, 3 \\ X_i &= a_i + p_2 \cos \theta_i - q_2 \sin \theta_i, Y_i = b_i + p_2 \sin \theta_i + q_2 \cos \theta_i; i = 4, 5, 6 \end{aligned} \quad (1.2)$$

$(a_i, b_i)$  and  $\theta_i$  are the desired rigid body positions of the coupler defined by the coordinate of point  $A$  and the couple angle with respect to the ground frame  $XOY$ . The solution was first found at poles graphically and then extended to the whole design space using a numerical method. Three phase problems were also solved using this method.

Hong and Erdman [11] used a set of quadratic scalar equations similar to Wang and Sodhi's and introduced a synthesis method for planar and spherical four-bar linkages with side-link lengths adjustable. Their model directly generates a third-degree polynomial circle point curve for two-phase five position motion synthesis.

Russell and Sodhi [12] developed a synthesis method for planar adjustable geared five-bar mechanisms for multi-phase motion generation using constant length requirement of the crank links. The input crank was geared with the driven side-link and both moving pivots were made adjustable. The synthesis method is similar to the one based on adjustable dyad.

Russell and Sodhi also reported work on adjustable spatial motion-generation mechanism synthesis [13, 14]. They adjusted the moving pivot positions to generate two-phase and three-phase motions. Their method was based on the modified R-R and S-S



constraint equations. Using this method, spatial RRSS mechanisms can be synthesized to achieve phases of prescribed precise rigid body positions and rigid body positions with tolerances. They also presented a method for synthesizing adjustable RSSR-SS mechanisms to achieve phases of prescribed positions, velocities and accelerations [15].

#### *b. Multi-phase Path Generation*

Path generation is motion generation without coupler angle requirements. Complex number synthesis methods for motion generation can also be used for path generation except coupler angles are not specified but design variables. The details of these methods are therefore not provided. A brief summary of reported work on multi-phase path generation is given below.

Limited work was done on adjustable mechanisms for multiple path generation. Early synthesis methods for adjustable mechanisms were primarily graphical. Tao and Krishnamoorthy [16, 17] graphically synthesized a planar four-bar linkage to generate multiple coupler curves with one or two cusps or symmetrical curves with a double point.

McGovern and Sandor [19] developed complex number method to synthesize mechanisms with a fixed pivot position adjustable for multiple path generations. Shimojima *et al.* [21] also adjusted a fixed pivot position to generate a straight line and an L-shaped path. These methods are similar to the complex number method for multi-phase motion generation except there are two loop equations and the coupler angles are unknowns.

Multiple paths with special features were also synthesized. Huston and Kramer [20] applied complex number synthesis method to the Bobillier Theorem mechanisms and synthesized adjustable four-bar path generating mechanisms for multiple circular arcs

tangential at a common point. Chang [23] synthesized adjustable four-bar mechanisms generating multiple arcs with specified tangential velocities.

Russell and Sodhi [22] synthesized a special class of slider-crank linkages based on a basic adjustable driven side-link length four-bar linkage. The linkage's slider guide was two concentric arcs tangentially connected by a transition curve. This slider-crank linkage was able to generate multi-phase motions, paths, or functions without a physical adjustment to the linkage.

All above methods generate multi-phase point-to-point paths defined by limited number of precision points. Only Zhou and Ting [39] reported work on multi-phase continuous path generation. They adjusted the slider guider positions of a slider-crank linkage and employed an optimization method to find the optimum linkage. The synthesized linkage can generate multiple continuous paths tangential at a common point.

### *c. Multi-phase Function Generation*

Multi-phase function generation problems can also be solved by complex number method. By eliminating coupler angles in the loop equations, Freudenstein's equations [1] are obtained, which is mostly used for function generation. Adjustments for function generation linkages are preferred to be made to the link lengths since the fixed pivots are input and output axes that are usually not adjusted and adjusting the moving pivots is equivalent to adjusting the coupler link length.

In the area of adjustable linkages for function generation, published work is also limited. Mruthyunjaya and Raghavan [26] developed graphical methods for derivative synthesis of the adjustable four-bar mechanism for function generation. The methods permit synthesis of the adjustable four-bar linkage to satisfy up to third-order precision

conditions for generation of two specified functions. Ahmad and Waldron [24] presented synthesis techniques for planar four bar function generators having adjustable link lengths. The inversion method was used to design the function generators.

Funabashi et al. [5] presented general methods to design planar, spherical and spatial crank-length adjusting mechanisms which can change input–output relationships and also stop output motions. Structures of the crank-length adjusting mechanisms were obtained by a number synthesis, after analyzing the relations between the crank length and the displacement of a moving pair on the crank in the case where the pair moves along a straight line or an arc fixed on a rotating plane of the crank shaft. Some applications of the mechanisms to adjustable path and function generators were shown.

McGovern and Sandor [18] developed methods to synthesize adjustable mechanisms for function generation using complex variables with finitely separated precision points and higher order synthesis involving prescribed velocities, accelerations, and higher accelerations. The linkages considered are a four-bar, a geared five-bar, and a geared six-bar mechanism.

Naik and Amarnath [25] presented synthesis of adjustable four-bar function generators through five-bar loop closure equations operating in two phases to produce two specified functions. They adjusted the fixed pivot position of a four-bar mechanism by rotating one link of the five-bar mechanism about its ground pivot and holding it in a fixed position. A maximum of three precision points for each function were selected in the illustrative example.

All above methods intended to design adjustable mechanisms that generate prescribed positions exactly. This approach, however, is limited by its maximum number of specified positions. Mechanisms with one adjustment synthesized by these methods can achieve only one or two additional positions than their non-adjustable counterparts. To make the situation worse, these positions are divided into phases; each phase contains even less design positions. As a matter of fact, most of the references cited above solved problems with only two to three positions in each phase, which is usually not enough for industrial application.

On the other hand, positioning error exists almost everywhere in real mechanism practices. Manufacturing, assembly, joint clearance, normal wear, and deformation under static and dynamic loads all add error to the mechanism. It is impractical to eliminate the error and industrial applications can be satisfied when the error is limited in a range. Therefore, requiring the mechanism to pass through all design positions exactly is artificial and unnecessary. Without this requirement, the optimal synthesis method emerges.

### 1.3 Optimal Synthesis

There are generally two kinds of mechanism synthesis approaches. *Exact* (or *precision point*) *synthesis* requires the designed mechanism to pass through all desired positions exactly. Since no error is allowed between the desired and generated motions, the maximum number of design positions is limited. On the other hand, *approximate* (or *optimal*, sometimes also called *optimum*) *synthesis* allows some error, called *Structural Error*, between the generated and the desired motions – the designed mechanism approaches the desired motion approximately, thus there is no limitation on the number of

design positions. Structural Error is conventionally formulated as the sum of the squared distance between the desired and the generated motions, and then mathematically minimized to find the mechanism that gives the best approximation of the desired motion.

An increasing number of research works have been published in the area of optimal synthesis of mechanisms since 1960's when mathematical optimization tools were applied to kinematic synthesis. Today, after decades of development, this powerful technique has become a highly favored tool in mechanism design.

### 1.3.1 Procedure of Optimal Synthesis

The general process of optimal synthesis consists of three steps:

1. Modeling: Selecting independent design variables, formulating the structural error ( $E$ , the objective function to be minimized), and find all constraints.
2. Translating to standard form of optimization problem:
  - Minimize:  $E = F(\mathbf{x})$ ,
  - Subject to:  $\mathbf{g}(\mathbf{x}) \geq 0$ ;  $\mathbf{h}(\mathbf{x}) = 0$ .
 where  $\mathbf{x} = (x_1, x_2, x_3, \dots, x_m)^T$  is the design variable vector,  $F(\mathbf{x})$  is the objective Function, and  $\mathbf{g}(\mathbf{x})$  and  $\mathbf{h}(\mathbf{x})$  are constraints.
3. Optimization: Solve the problem for  $\mathbf{x}$  and  $E_{\min}$  using mathematic algorithms for the "best" mechanism that approximates the desired motion with the minimum error. The available optimization algorithms include traditional gradient-based methods such Linear Search, Quasi-Newton Method, Gauss-Newton Method, etc. and modern probability-based or evolutionary methods such as Simulated Annealing, Genetic Algorithm, etc.

### 1.3.2 Structural Error

The conventional structural error evaluates the error between generated and desired motions directly. For path generation as an example, as shown in Figure 1.3, the distance between the desired and the generated paths is calculated at selected points and is then squared and added up:

$$E = \sum_{j=1}^n [(x_{dj} - x_{gj})^2 + (y_{dj} - y_{gj})^2] \quad (1.3)$$

where  $n$  is the number of design points. For optimal path generation, the desired path are usually given by a set of path points  $(x_{dj}, y_{dj})$ .

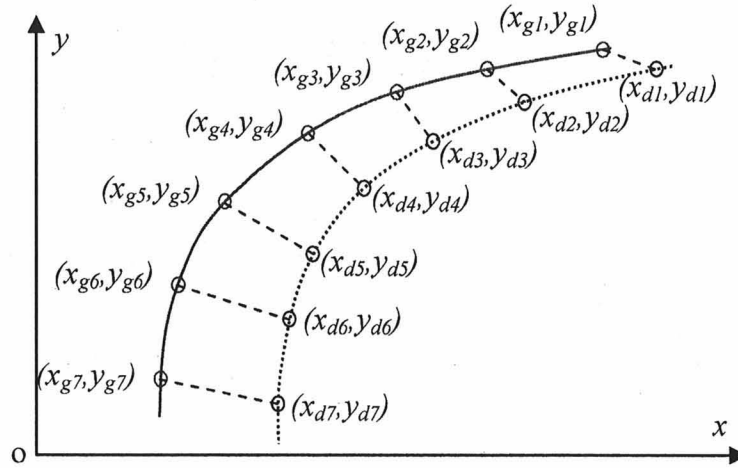


**Figure 1.3** The desired and generated paths.

The generated path point  $(x_{gj}, y_{gj})$  is calculated at the corresponding input crank angle, which are also design variables. Take the four-bar linkage in Figure 1.4 as an example, the design variables are  $x=(x_0, y_0, r_1, r_2, r_3, r_4, r_{cx}, r_{cy}, \theta_0, \theta_{2j}), j=1, 2, \dots, n$ , the coordinates of the coupler point  $C$  in the local frame is given by

$$\begin{aligned} C_{x_{rj}} &= r_2 \cos \theta_{2j} + r_{cx} \cos \theta_{3j} - r_{cy} \sin \theta_{3j} \\ C_{y_{rj}} &= r_2 \sin \theta_{2j} + r_{cx} \sin \theta_{3j} - r_{cy} \cos \theta_{3j} \end{aligned} \quad (1.4)$$

where  $\theta_{3j}$  can be found by solving

$$\begin{aligned} r_2 \sin \theta_{2j} + r_3 \sin \theta_{3j} &= r_4 \sin \theta_{4j} \\ r_2 \cos \theta_{2j} + r_3 \cos \theta_{3j} &= r_1 + r_4 \cos \theta_{4j} \end{aligned} \quad (1.5)$$

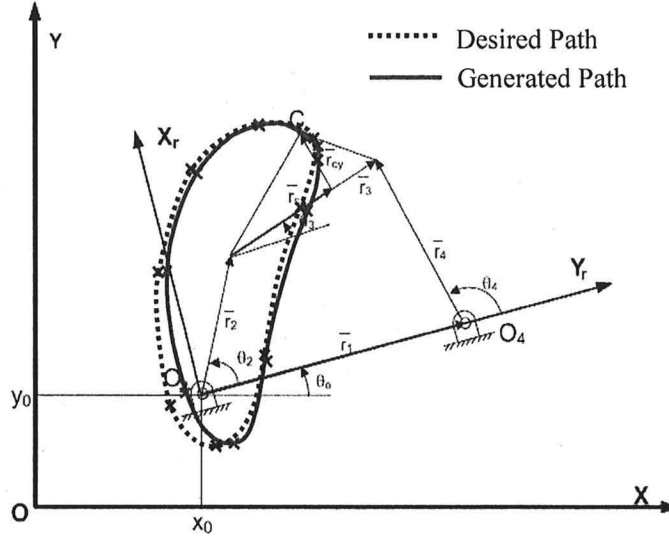


**Figure 1.4** Optimal path generation of a four-bar linkage.

$\theta_{4j}$  is eliminated so that  $\theta_{3j}$  is solved as a function of  $\theta_{2j}$ . When mapped back to the global coordinate system,

$$\begin{bmatrix} x_{gj} \\ y_{gj} \end{bmatrix} = \begin{bmatrix} C_{Xj} \\ C_{Yj} \end{bmatrix} = \begin{bmatrix} \cos \theta_0 & -\sin \theta_0 \\ \sin \theta_0 & \cos \theta_0 \end{bmatrix} \begin{bmatrix} C_{Xrj} \\ C_{Yrj} \end{bmatrix} + \begin{bmatrix} x_0 \\ y_0 \end{bmatrix} \quad (1.6)$$

Substitute Eq. (1.6) into Eq. (1.3), the resulted structural error is a highly nonlinear function with high order polynomials and trigonometric functions of a large number ( $n+9$ ) of unknowns. More unknowns result in larger search space; high nonlinearity structural

error adds more difficulty to the optimization process because numerical method has to be used to approximate its gradient vector and Hessian matrix.

### 1.3.3 Optimal Synthesis Methods

Research on optimal synthesis falls into two aspects: (1) finding new approaches of modeling the problem to construct different forms of structural error on various design variables, and (2) applying different and newly-developed optimization methods to solve the modeled problem.

#### *a. Alternative Structural Errors*

Several researchers have made effort to formulate alternative forms of structural error. One early attempt was by Angeles *et al.* [27] who implemented another optimization to find the input angle that provides the least distance between the generated coupler curve and each design point. This method avoided using input crank angles as design variables and thus uses fewer variables, in the cost of additional computation of the optimized input angle. Watanabe [29] used the maximum of absolute values of curvature differences between the two paths, expressed as an equation of the arc length, as the objective function. Comparison points were selected on the two paths with equal arc length interval.

Vallejo [37] first introduced a new idea of forming indirect structural error based on deformation of the linkage. In his model, the whole linkage was considered “deformable” or “flexible”: the linkage was able to deform (links being elongated or shortened) to allow its coupler point to reach a point that it cannot reach at the linkage’s original dimensions, as shown in Figure 1.5. Deformation energy was then stored in the “elastic” links. An optimization process found the optimal linkage parameters that minimize the sum of deformation energies at all design points, as in Eq. (1.7). This is a novel and reasonable



method of constructing the structural error, but it still suffers from heavy computation: since the mechanism is not a structure but a system of at least one degree of freedom, the calculation of the deformation energy also needs an optimization process; and the solved energy function is also nonlinear.

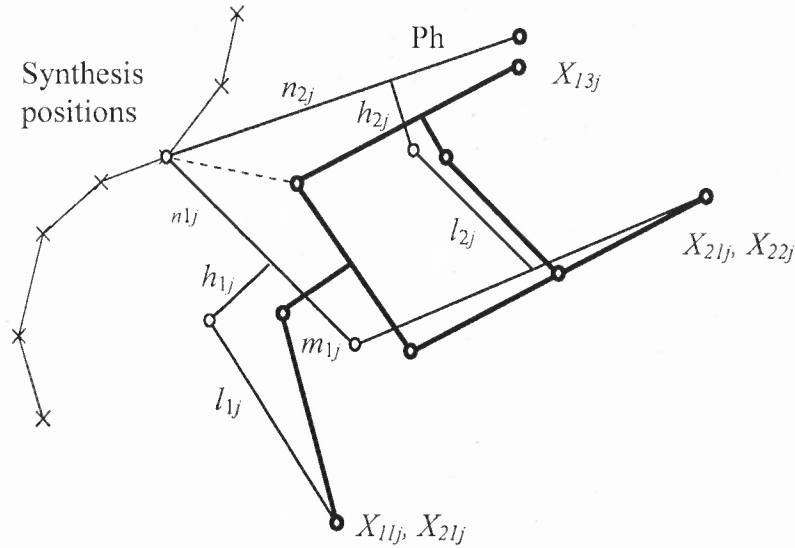


**Figure 1.5** A deformable linkage model.

$$\Phi = \Phi_h + \Phi_t + \Phi_f = \sum_{j=1}^N w_i \left[ \sum_{i=1}^h (l_{ij} - L_i)^2 + \sum_{i=1}^t \left[ 2 \cdot (h_{ij} - H_i)^2 + (m_{ij} - M_i)^2 + (n_{ij} - N_i)^2 + (d_{ij} - D_i)^2 \right] + \sum_{i=1}^f (x_{rij} - X_{ri})^2 \right] \quad (1.7)$$

Zhou simplified Vallejo's method by making only one of the linkage's parameters flexible: the fixed pivot of a four-bar linkage [38] or slider guider position of a slider-rocker linkage [39]. When the coupler point traces the desired path exactly, the error of the linkage is then transferred to the flexible parameter.

As shown in Figure 1.6, the ground joint  $D$  is freed from the ground link while still connecting link  $AD$  and  $CD$ . Since the current linkage dimension is not likely to be able to generate the desired path  $K$  exactly, when the coupler point  $M$  is forced to move along the desired path, joint  $D$  will rotate about the still-fixed ground joint  $A$ , or in other words, the angle  $\varphi$  varies between  $\varphi_{\max}$  and  $\varphi_{\min}$ . The structural error, called *Orientation Structural Error* of the fixed link, is then defined as

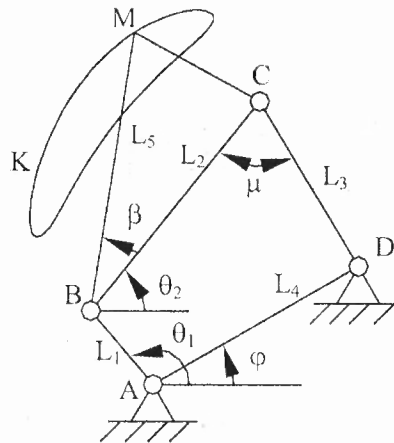


**Figure 1.6** A four-bar crank-rocker path generation linkage.

Source: H. Zhou and E. H. M. Cheung, Optimal synthesis of crank-rocker linkages for path generation using the orientation structural error of the fixed link, *Mechanism and Machine Theory* 36 (2001) 973-982.

$$E_s = \varphi_{\max} - \varphi_{\min} \quad (1.8)$$

Figure 1.7 shows the driving dyad of the linkage. The angle  $\varphi$  is calculated as following. Since the driving crank needs to make a full turn in a preferred crank-rocker linkage, the link lengths  $L_1$  and  $L_5$  must satisfy the following conditions:

$$\begin{aligned} L_1 + L_5 &= R_{\max} \\ |L_1 - L_5| &= R_{\min} \end{aligned} \quad (1.9)$$

where  $R_{\max}$  and  $R_{\min}$  can be found from the given path and the yet unknown ground joint  $A(x_A, y_A)$ , hence  $L_1$  and  $L_5$  are no longer independent. The independent design variables are  $\mathbf{X} = (x_A, y_A, L_2, L_3, L_4, \beta)^T$ . The value of angle  $\theta_1$  and  $\theta_3$  can be then obtained as

$$\theta_1 = \tan^{-1} \left( \frac{y_M - y_A}{x_M - x_A} \right) \pm \cos^{-1} \left( \frac{L_1^2 + (x_M - x_A)^2 + (y_M - y_A)^2 - L_5^2}{2L_1 \sqrt{(x_M - x_A)^2 + (y_M - y_A)^2}} \right) \quad (1.10)$$

where

$$\theta_5 = \tan^{-1} \left( \frac{y_M - y_A - L_1 \sin \theta_1}{x_M - x_A - L_1 \cos \theta_1} \right) \quad (1.11)$$

The  $\pm$  sign in Eq. (1.16) corresponds to the two rotation direction of the crank  $AB$ .

The angle  $\theta_2$  is then

$$\theta_2 = \theta_5 - \beta \quad (1.12)$$

Coordinates of joint C can be then obtained as

$$\begin{aligned} x_C &= x_A + L_1 \cos \theta_1 + L_2 \cos \theta_2 \\ y_C &= y_A + L_1 \sin \theta_1 + L_2 \sin \theta_2 \end{aligned} \quad (1.13)$$

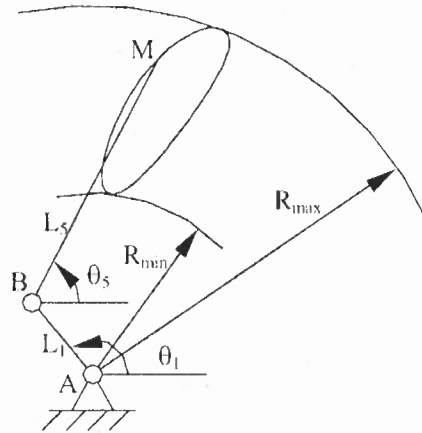


**Figure 1.7** The driving dyad of the four-bar path generator.

Source: H. Zhou and E. H. M. Cheung, Optimal synthesis of crank-rocker linkages for path generation using the orientation structural error of the fixed link, *Mechanism and Machine Theory* 36 (2001) 973-982.

Finally the angle of the link  $AD$  is given by

$$\varphi = \tan^{-1} \left( \frac{y_C - y_A}{x_C - x_A} \right) - \cos^{-1} \left( \frac{L_4^2 + (x_C - x_A)^2 + (y_C - y_A)^2 - L_3^2}{2L \sqrt{(x_C - x_A)^2 + (y_C - y_M)^2}} \right) \quad (1.14)$$

Although this optimization model needs only five scalar unknowns, the structural error function is still complicated.

Lioa, Cossalter, and Lot [44] used natural coordinates to model the mechanism and their performance function (structural error) consisted of the residual of the motion generation requirement equations written in natural coordinates. This method resulted in a simpler merit function for optimization, but the modeling with natural coordinates was a case-by-case approach that needs extra effort for different mechanisms.

Ullah and Kota [45] used Fourier Descriptors to evaluate only the shape of the desired and generated paths to avoid optimizing the shape, size, and orientation of the linkage at the same time. The synthesized linkage was then scaled and rotated to match the desired path. Kim and Sodhi [30] made the coupler point pass through five specified points on the path exactly and optimized the fixed pivot position of the driving crank to minimize the overall error at other points. The disadvantage of this method is the error of driven side link length was used in a special form that needs to be solved from a system of equations.

#### *b. Optimization Methods*

Most work on optimal mechanism design was based on traditional gradient-based optimization algorithms. To name a couple, Mariappan [31] and Sancibrian [32] developed exact-gradient based methods for optimal path synthesis. The former presented a general form of exact gradient functions of a conventional structural error for optimal path generation. The later used a specific formulation to obtain the exact elements of the gradients, and sensitivity parameters for all the design variables were determined giving a first order relationship between the parameters of interest. However, with this formulation the explicit expression of the structural error itself was difficult to obtain, thus a first order Taylor series approximation was used. This information was used in the optimization algorithm to enhance the convergence rate.

Least square method was developed to solve linear or nonlinear systems approximately when an exact solution either does not exist or is too difficult to find. When applied to mechanism synthesis, the residuals of design equations are squared and added up in a least square sense and then the gradient equations of the residual are solved to find the minimum of this sum as well as values of design variables that give this minimum. This

method, however, is not able to handle constraints. Angeles *et al* applied unconstrained nonlinear least square method to planar motion [42] and path [43] generation linkages. Russell and Sodhi [27] used least square method for motion generation of adjustable five bar spherical mechanisms. Gradient equations were solved numerically to find the possible minima.

Applications of new optimization algorithms to mechanism synthesis have also been carried out. Modern optimization methods such as Ant-gradient Search [34], Fuzzy Logic [35], Tabu-Gradient Search [41] were recently introduced to optimal kinematic synthesis problems to find the global minimum. Evolutionary genetic algorithm (GA) [33] is used to find the global minimum of the optimization problem without deep understanding and adjustment of the problem itself. Self-learning *Neural Network* [36] is also a powerful tool in optimal mechanism design. Hoeltzel and Chieng [28] developed a pattern matching method based on the neural network model of pattern of coupler curves according to moment variants.

#### **1.4 Research Objectives**

All of the reported synthesis methods for adjustable mechanisms are focused on achieving additional phases of precision positions or special features from the adjustment except in [39]. For exact synthesis, however, the advantage of adjustments is limited. One adjustment to the linkage adds only one or two scalar design variables, which in return provides one or two additional design positions. Furthermore, the adjustment divides those design positions into two or more phases, each of which contains even fewer design positions, making adjustable mechanisms less desirable.

To extend the capability of adjustable mechanisms, optimization methods need to be employed. With optimal or approximate synthesis, each phase of adjustable mechanisms can achieve considerably more design positions with an acceptable error. Although optimal synthesis is a well-explored field in which many synthesis methods have been developed, there are few applications of optimal synthesis methods to adjustable mechanisms. The only work on optimal synthesis of adjustable mechanisms was reported by Zhou and Ting [39], whose method is only capable of generating a series of tangential curves.

The objective of this research is to develop a generalized optimal synthesis method for adjustable planar linkages for multi-phase motion, path, and function generation for the first time. Since the existing optimal synthesis methods will result in a complicated structural error function of too many design variables when applied to adjustable mechanisms with many design positions in each phase, new optimal synthesis method suitable to adjustable mechanisms needs to be developed. The deformation energy method developed by Vellejo et al needs to be simplified to provide a compact and easy-to-calculate structural error which consists of less design variables and can be applied to different synthesis tasks. The next chapter will present an optimal synthesis method based on link length structural error. When applied to multi-phase motion, path, and function generation, minor modifications need to be made according to the requirement of the problems. The following chapters examine the application of this method to optimal multi-phase motion, path, and function generation and present formulated synthesis models and equations case by case.

**CHAPTER 2**  
**OPTIMAL SYNTHESIS BASED ON**  
**LINK LENGTH STRUCTURAL ERROR**

**2.1 Link Length Structural Error**

**2.1.1 Formulation**

As discussed in Chapter 1, the conventional structural error is not suitable for optimal adjustable mechanism design for its high nonlinearity and unavailable gradient vector and Hessian matrix. The several alternative forms of structural error are either too difficult to construct or lack of generality.

To construct a more simplified and generalized form of structural error, we start from the motion generation problem. Given desired coupler points  $P_i$  and coupler angles  $\theta_{5i}$ , the objective of motion generation is to find two or more dyads that guides the coupler through the given rigid body positions.

Motion synthesis is to find a circle point (moving pivot) on the moving plane (coupler) which keeps a constant distance to a center point (fixed pivot) on the fixed plane (ground link) at all prescribed rigid body positions of the coupler. For more than five prescribed positions for a four-bar linkage, such points may not exist. The distance between any given moving point  $C$  and some fixed point  $D$  fluctuates around a constant value while the coupler link moves through the prescribed positions. If the link length of  $CD$  is considered flexible, this fluctuation can be called *link length structural error*. Taking this moving point as the circle point and the corresponding fixed point as the center point, the dyad will be able to move its coupler through the given positions with some error. The



smaller the link length structural error, the smaller is the error between the generated and desired motions. When this structural error is zero, the resulted dyad would guide the rigid body through all the desired positions exactly. Therefore this structural error effectively represents the overall error of the generated motion. We minimize the link length structural error to find the best circle and center points.

Link length structural error can be considered as a simplified form of Vallejo's deformation energy error function [37]. By using only one link length as the flexible parameter of the whole linkage, optimization is not needed to calculate the deformation energy and the error function is much easier to construct and has a compact fourth order polynomial form, which is easy to minimize since its explicit form of gradient vector and Hessian matrix are available.

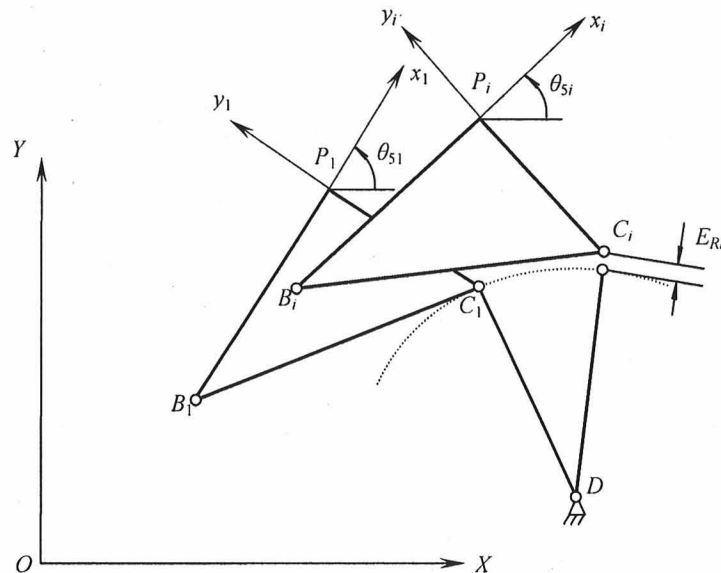


**Figure 2.1** The link length structural error.

As shown in Figure 2.1, coupler link  $BPC$  moves through positions given by the desired path points  $P_i(x_i, y_i)$  and coupler angles  $\theta_{5i}$  with respect to the global coordinate system  $XOY$ . The local coordinate system  $X_iP_iY_i$  is located at tracing point  $P$  with its  $x$  axis in the direction of  $BP$  and moves with the moving plane.

The global coordinates (in frame  $XOY$ ) of the moving pivot  $C$  at their first design positions,  $C_1$ , and the coordinates of the fixed pivot  $D$ , are taken as design variables,

$$C_1 = (x_{C1}, y_{C1})^T, D = (x_D, y_D)^T, \quad (2.1)$$

Coordinates of joint  $C$  at other design positions  $C_i$  can be found by

$$C_i = (x_{C_i}, y_{C_i})^T, (x_{C_i}, y_{C_i}, 1)^T = T_{1i}(x_{C1}, y_{C1}, 1)^T \quad (2.2)$$

where  $i=2, 3, 4, \dots, n$ ,  $T_{1i}$  is the coordinate transformation matrix from frame  $X_1P_1Y_1$  to frame  $X_iP_iY_i$ ,

$$T_{1i} = \begin{bmatrix} \cos(\theta_{5i} - \theta_{51}) & -\sin(\theta_{5i} - \theta_{51}) & -\cos(\theta_{5i} - \theta_{51})x_1 + \sin(\theta_{5i} - \theta_{51})y_1 + x_i \\ \sin(\theta_{5i} - \theta_{51}) & \cos(\theta_{5i} - \theta_{51}) & -\sin(\theta_{5i} - \theta_{51})x_1 - \cos(\theta_{5i} - \theta_{51})y_1 + y_i \\ 0 & 0 & 1 \end{bmatrix} \quad (2.3)$$

The side-link length structural error can be given as

$$E_R = \sum_{i=2}^n \eta_i [(C_i - D)^T (C_i - D) - (C_1 - D)^T (C_1 - D)]^2 \quad (2.4)$$

where  $\eta_i$  is a weighting coefficient for each design points. For points that require more accuracy, a large  $\eta_i$  is given.

Since two dyads are needed to form a four-bar linkage, there are two approaches available to synthesis the whole linkage. One is to find several local minimums of the structural error in Eq. (2.4). An easy way to do this is to repeatedly pick different points (meshing the space into grids and sequentially picking the nodes could be a simple approach) within the design space as the initial guess for the unknown  $C_1$  or  $D$  and do the local minimum search. Most likely these optimization processes with different initial guess will converge at several optimized dyads. Then two of these optimal dyads can be picked as two sides of the synthesized four-bar linkage, according to the design constraints such as the Grashof's condition, link length and space restrictions, transmission angle requirement, etc. This method, however, is computation demanding.

The other approach is to add the second dyad to the structural error. For the other dyad  $ABP$ , the same structural error can be given as

$$E_R' = \sum_{i=2}^n \mu_i [(B_i - A)^T (B_i - A) - (B_1 - A)^T (B_1 - A)]^2 \quad (2.5)$$

The overall link length structural error is then

$$E_R = \sum_{i=2}^n \{ \mu_i [(B_i - A)^T (B_i - A) - (B_1 - A)^T (B_1 - A)]^2 + \eta_i [(C_i - D)^T (C_i - D) - (C_1 - D)^T (C_1 - D)] \} \quad (2.6)$$

The structural error  $E_R$  formulated is a fourth order polynomial of only four scalar unknowns ( $x_{C1}, y_{C1}, x_D, y_D$ ) for single-dyad optimization or eight unknowns ( $x_{C1}, y_{C1}, x_D, y_D, x_{B1}, y_{B1}, x_A, y_A$ ) for both dyads, no matter how many design positions are prescribed, compared to the conventional structural error that would have  $n+3$  unknowns. Also, no crank angles are included in the structural error, which makes the calculation of gradient simpler.

Equation (2.6) is developed for optimal motion generation. For path generation, simply let the coupler angles in Eq. (2.4) or Eq. (2.6) be unknowns; the expression of the structural error is the same. The resulted structural error function is still much simpler than the conventional one.

### 2.1.2 Validation

In order to prove that when the indirect link length structural error is small, the conventional structural error formulated by directly comparing the two motions is also small, one needs to prove that the link length structural error is an infinitesimal of the same or lower order than the conventional structural error, which means the link length structural error approaches zero slower than the conventional one so that when it is minimized to a small value, the conventional structural error is also small.

For a four-bar linkage synthesized by minimizing the link length structural error in Eq. (2.6) as drawn in Figure 2.2, for the driven dyad, suppose  $BCP$  is the desired coupler position and because of the length error  $\Delta R$  of the link  $CD$  ( $\Delta R$  is considered an infinitesimal compared with the link lengths of the linkage), the coupler is moved to its actual position  $BC'P'$ . Here the joint B is not movable, assuming the driving dyad has no error.

Since a transmission angle constraint is usually applied to the driven dyad, link  $BC$  and  $CD$  are not collinear. For triangular  $\triangle BCD$ , the law of cosines gives

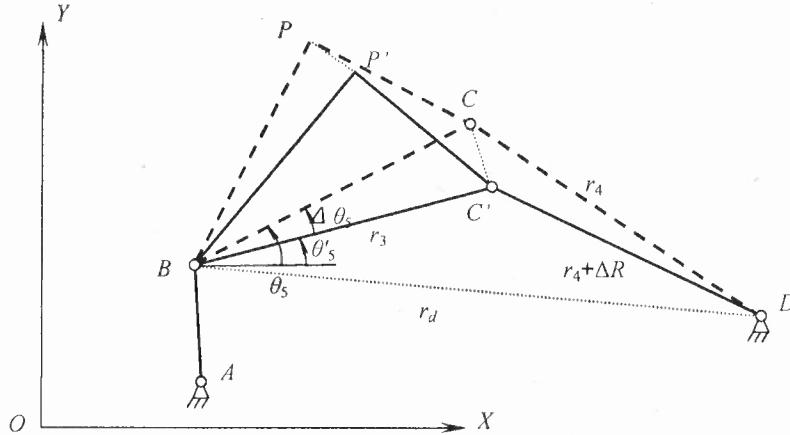


**Figure 2.2** A four-bar linkage with a driven-side link length error.

$$\cos \angle CBD = \frac{r_3^2 + r_d^2 - r_4^2}{2r_3r_d} \quad (2.7)$$

Giving  $r_4$  a small change  $\Delta R$  yields

$$\cos \angle C'BD = \frac{r_3^2 + r_d^2 - (r_4 + \Delta R)^2}{2r_3r_d} = \cos \angle CBD - \frac{2r_4\Delta R + \Delta R^2}{2r_3r_d} \quad (2.8)$$

Therefore, the change of cosine of the coupler angle is

$$\cos \angle C'BD - \cos \angle CBD = -\frac{2r_d \Delta R + \Delta R^2}{2r_3 r_d} = O(\Delta R / r_d) \quad (2.9)$$

As shown in Eq. (2.11), it can be proven that  $\Delta\theta_5$  is an infinitesimal of the same order as  $\cos \angle C'BD - \cos \angle CBD$ , so  $\Delta\theta_5$  is a same order infinitesimal as  $\Delta R / r_d$ , so is  $PP'$ :

$$\Delta\theta_5 = O(\Delta R / r_d), PP' \approx BP \cdot \Delta\theta_5 = \Delta R \quad (2.10)$$

$$\begin{aligned} \lim_{\Delta\theta_5 \rightarrow 0} \frac{\cos \angle C'BD - \cos \angle CBD}{\Delta\theta_5} &= \lim_{\Delta\theta_5 \rightarrow 0} \frac{\cos(\theta - \Delta\theta_5) - \cos \theta}{\Delta\theta_5} \\ &= \lim_{\Delta\theta_5 \rightarrow 0} \frac{\cos \theta \cos \Delta\theta_5 - \sin \theta \sin \Delta\theta_5 - \cos \theta}{\Delta\theta_5} = \lim_{\Delta\theta_5 \rightarrow 0} \frac{\cos \theta (\cos \Delta\theta_5 - 1) - \sin \theta \sin \Delta\theta_5}{\Delta\theta_5} \\ &= \lim_{\Delta\theta_5 \rightarrow 0} \frac{\cos \theta (\cos \Delta\theta_5 - 1)}{\Delta\theta_5} - \lim_{\Delta\theta_5 \rightarrow 0} \frac{\sin \theta \sin \Delta\theta_5}{\Delta\theta_5} = \lim_{\Delta\theta_5 \rightarrow 0} \frac{\cos \theta [\frac{1}{2}(\Delta\theta_5)^2]}{\Delta\theta_5} - \lim_{\Delta\theta_5 \rightarrow 0} \frac{\Delta\theta_5 \sin \theta}{\Delta\theta_5} \\ &= -\sin \theta \end{aligned} \quad (2.11)$$

Here the current coupler angle  $\theta$  is a known constant usually constrained within a range such as  $[45^\circ, 135^\circ]$ , so  $-1 < -\sin \theta < 0$ , which means  $\Delta\theta_5$  is an infinitesimal of the same order as  $\cos \angle C'BD - \cos \angle CBD$ .

This indicates that with a transmission angle constraint, or in other words, when link  $BC$  and  $CD$  are not collinear, the link length structural error is as effective as the conventional one. For the driving dyad which has no transmission angle requirement applied, difficulties appear when the link  $AB$  and  $BC$  are collinear, as shown in Figure 2.3.

Since any position from the movement of the coupler link can be chosen as the generated position, the following arrangements are made to fit this situation: the other side-link  $CD$  is set movable and the generated position is chosen such that the link  $B'C'$  is still in line with link  $AB'$  when the link length error  $\Delta R$  is applied. Therefore the law of cosines can be applied to triangular  $ACD$  and prove that  $\angle C'DC$  is again an infinitesimal of the same order of  $\Delta R$ , so is the length of  $CC'$ . The angle  $\angle C'AC$  is then a same order infinitesimal too. Thus the difference between the generated coupler position  $B'C'P'$  and the desired one  $BCP$  is of the same order of  $\Delta R$ .

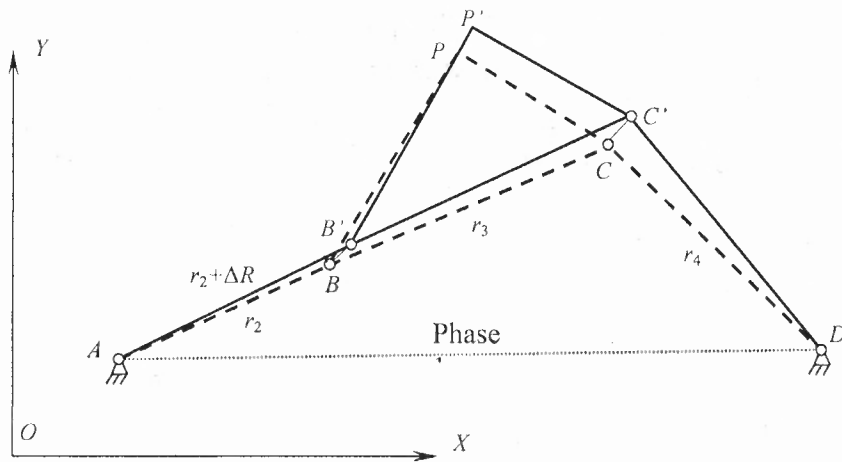


**Figure 2.3** A four-bar linkage with a driving crank length error.

For both dyads combined, the sum of these two infinitesimal is a same order infinitesimal. Thus the link length structural error is proven to be equivalent to the conventional structural error for motion and path generation. The validation for planar function generation will be given in Chapter 5.

## 2.2 Optimization Model

With eight scalar unknowns ( $x_{C1}$ ,  $y_{C1}$ ,  $x_D$ ,  $y_D$ ,  $x_{B1}$ ,  $y_{B1}$ ,  $x_A$ ,  $y_A$ ) for a four-bar motion generation problem, The optimal synthesis problem becomes:

Minimize:  $E_R$  in (2.6)

Subject to the following constraints:

### a. Grashof's Criterion

Grashof's criterion is applied when a Grashof's linkage is preferred. Suppose link  $AB$  is to be the input crank, then it is preferred to be the shortest link of this linkage because a crank-rocker is usually desired. The longest link is not determined yet, thus a general form of Grashof's condition can be given as  $AB + r_l < r_p + r_q$ .

### b. Transmission Angle

Given coordinates of pivots  $B$ ,  $C$  and  $D$ , the transmission angle  $\mu$  ( $\angle BCD$ ) can be easily calculated. The transmission angle is limited to  $\mu_{\min} < \mu < \mu_{\max}$ .

### c. Link Lengths

At least one positive length constraint has to be imposed to link  $AD$  or  $BC$ , otherwise the algorithm will converge to a solution whose dyad  $ABP$  and  $CDP$  are identical. Other constraints can be applied by restricting joint coordinates in suitable ranges.

### d. Order Constraint

Order requirement is associated with the input crank angle at all design positions. The input angle can be obtained by

$$\theta_{li} = \tan^{-1} \left( \frac{y_{Bi} - y_C}{x_{Bi} - x_C} \right), \quad -\pi/2 < \theta_{li} < \pi/2 \quad (2.11)$$



For  $\theta_{1i}$  out of this range,  $\pi$  should be added. Depending on the crank's rotating direction, the order constraints can be applied as

$$\theta_{1i} - \theta_{1(i+1)} < 0 \text{ or } \theta_{1i} - \theta_{1(i+1)} > 0, i=1,2,\dots,n, \quad (2.12)$$

### 2.3 Optimization Algorithm

Due to the small number of design variables, simple forms of constraints, and polynomial form of structural error, conventional gradient-based optimization methods can effectively solve this optimization problem. However, if the global minimum is required, other optimization algorithms need to be used.

Though various gradient-based algorithms can be employed to solve the standardized optimization problem, *Sequential Quadratic Programming* (SQP) is chosen for its robustness and efficiency. All numerical examples in this research are solved with Matlab R2006a's Optimization Toolbox, which has SQP implemented in.

As a generalized Newton's method, Sequential Quadratic Programming attempts to find the search direction from the current point by minimizing a quadratic sub-problem and then do a one-dimensional search for the next point. This method, however, finds the local minimum and its solution depends on the initial guess.

When equality and inequality constraints are both considered, the formulation of a nonlinear programming problem can be given by:

Minimize:  $f(x)$

Subject to:  $h(x) = 0$  and  $g(x) \leq 0$

The nonlinear programming formulation can be converted into a Lagrangian augment function form:

$$L = f(x) + \lambda^T h(x) + \zeta^T g(x) \quad (2.13)$$

where  $\lambda$  and  $\zeta$  are the Lagrangian multiplier vectors for the equality constraints  $h$  and the inequality constraints  $g$ , respectively. The correspondent Quadratic Programming problem is expressed as:

Minimize:

$$Q(s) = \nabla f^T s + \frac{1}{2} s^T (\nabla^2 L) s \quad (2.14)$$

Subject to:

$$\begin{aligned} \nabla g^T s + g &\leq 0 \\ \nabla h^T s + h &= 0 \end{aligned} \quad (2.20)$$

Through solving the above quadratic programming problem, the search direction  $s$  is determined. Then the problem becomes a one-dimensional search problem, which can be solved using exterior penalty function method, as:

Minimize

$$\Phi = f(x) + \sum_{j=1}^m \lambda_j \max(0, g_j(x)) + \sum_{k=1}^p \zeta_k |h_k(x)| \quad (2.15)$$

where  $x^{q+1} = x^q + \alpha s$ ,  $s$  is obtained by QP process above.

The diagram of SQP can be given as in Figure 2.4. During the optimization process, the Hessian matrix  $H = \nabla^2 L$  needs to be updated at each iteration. The most popular and useful method to generate an approximate Hessian matrix is the Broyden-Fletcher-Goldfarb-Shanno (BFGS) method (as Matlab uses), by which a positive definite Quasi-Newton approximation of the Hessian of the Lagrangian function,  $\mathbf{H}$ , is given by

$$H^{q+1} = H^q + \frac{\phi^q (\phi^q)^T}{(\phi^q)^T \alpha s^q} - \frac{(H^q)^T (\alpha s^q)^T \alpha s^q H^q}{(\alpha s^q)^T H^q \alpha s^q} \quad (2.16)$$

where  $\phi^q = \Phi^{q+1} - \Phi^q$ .

Numerical approximation of the Hessian matrix obviously adds computing time and decrease the convergence rate of SQP. Using the optimization model formulated in Section 2.3, however, the expression of an explicit form of the Hessian matrix of the goal function and constraints can be given to avoid numerical approximation, which is one of the major advantages of the proposed optimal synthesis method.

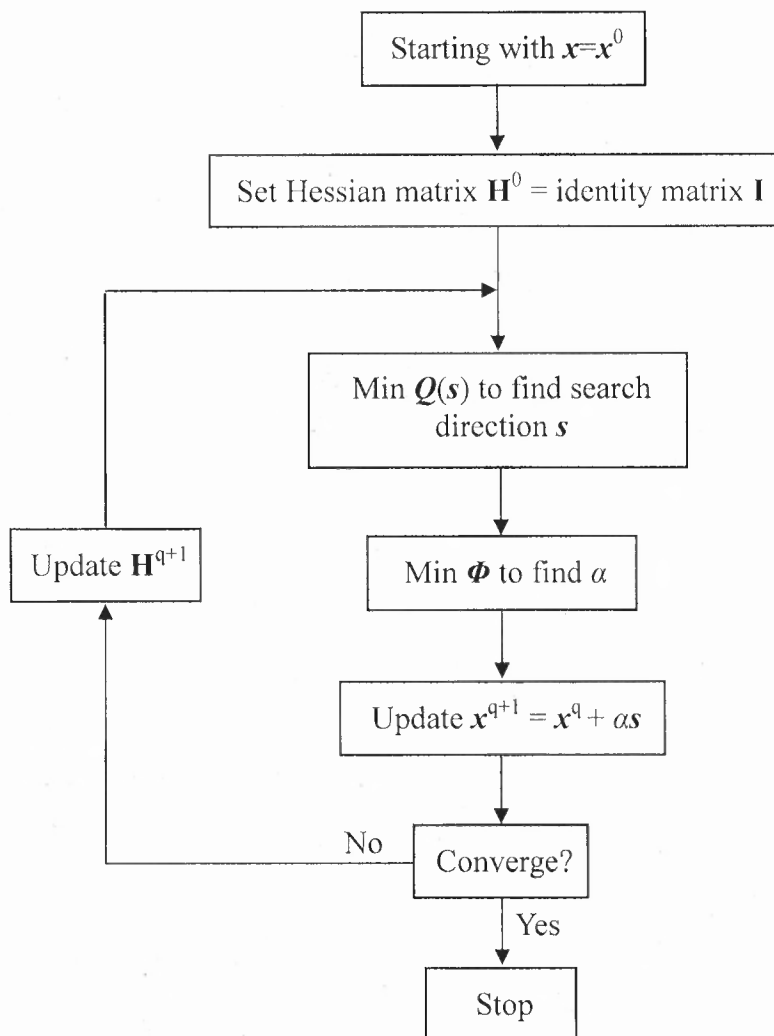


**Figure 2.4** Diagram of Sequential Quadratic Programming algorithm.

## 2.4 Synthesis Examples

Two numerical examples are synthesized below, one for motion generation and one for path generation. Both examples have at least 20 design positions, which are much more than what a four-bar linkage can precisely generate.

### 2.4.1 Optimal Motion Generation

21 rigid body positions along a “half-hearted” curve are to be passed through by the coupler of a four-bar linkage with minimum error. The desired positions are listed in Table 2.1. The coordinates of linkage joints are restricted within the range  $[-20, 20]$ .

Equation (2.4) is used for the structural error and points within the design space are used repeatedly as the initial guess of the joint  $C$  and  $D$  with an increment of 5.0 in the  $x$  and  $y$  coordinates. The totally  $9^4=6561$  optimizations starting from different initial guess are found to converge at several local minimums, or local optimal dyads, as the first five of which are listed in Table 2.2. Among these five dyads, the number one and three are chosen to form a crank-rocker, according to Grashof’s criteria. The synthesis four-bar linkage joint coordinates are listed in Table 2.3 and the linkage with the desired and generated positions was shown in Figure 2.5. The generated rigid body positions are approximately chosen from the continuous motion generated by the resulted linkage. The computing time for a local search is less than 1 second on a Pentium 4 PC, and the repeated search lasted about 11 minutes.

**Table 2.1** Desired and Generated Positions

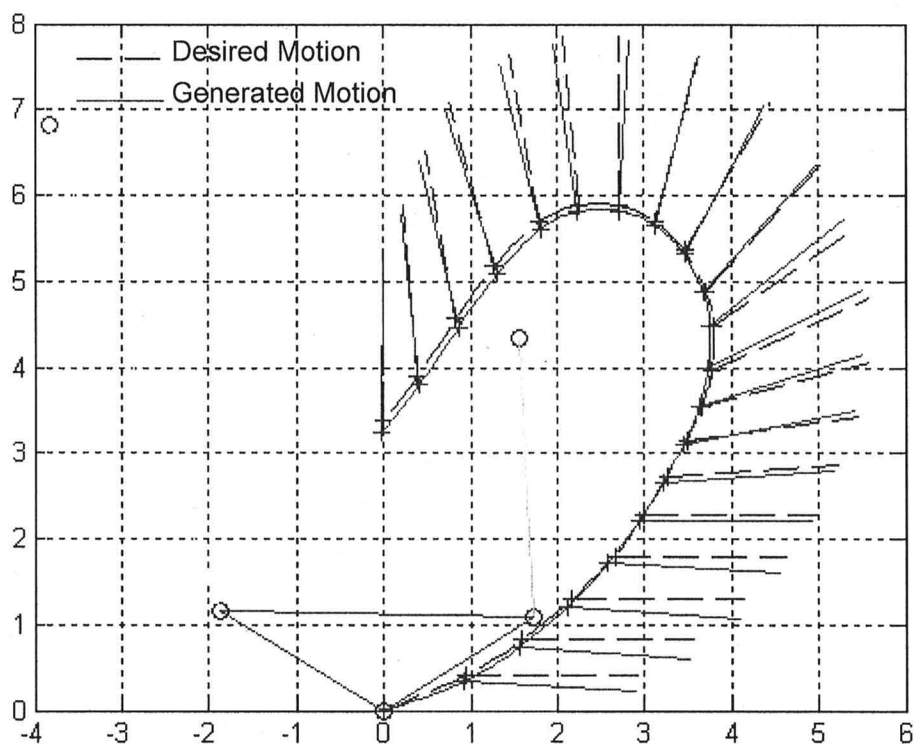
Desired Motion		Generated Motion	
Couple Point	Coupler Angle	Coupler Point	Coupler Angle
0,0	0	0.0,0.0	0.0
0.9356,0.4064	0	0.9156,0.3364	-3.1
1.5983,0.8220	0	1.5583,0.7320	-4.0
2.1704,1.3002	0	2.1204,1.2102	-4.5
2.6621,1.7986	0	2.5821,1.7186	-2.8
2.9957,2.2692	0	2.9457,2.2092	0.1
3.2614,2.7276	4	3.2214,2.6476	4.3
3.4941,3.1408	8	3.4641,3.1108	1.7
3.6635,3.5485	15	3.6335,3.5385	18.4
3.7798,3.9623	25	3.7398,3.9823	27.5
3.7992,4.4734	35	3.7592,4.4734	39.7
3.7170,4.8783	48	3.6847,4.8683	49.1
3.4675,5.3624	60	3.4675,5.3124	62.8
3.1242,5.698	75	3.1242,5.6486	76.5
2.7158,5.8800	90	2.7158,5.8200	87.9
2.2517,5.8780	95	2.2417,5.8080	98.0
1.7997,5.6882	100	1.8197,5.6082	104.1
1.2732,5.1741	105	1.3032,5.0841	107.4
0.8336,4.5628	100	0.8636,4.4628	103.1
0.4003,3.9064	95	0.4103,3.7964	96.7
0,3.3800	90	-0.0258,3.2407	89.8

**Table 2.2** First 5 Local Minimums

	$C_{lx}$	$C_{ly}$	$D_x$	$D_y$	$E_R$
1	1.7238	1.0819	1.5630	4.3296	0.5742
2	2.3367	1.3524	2.0562	4.8018	0.9018
3	-1.8743	1.1612	-3.8165	6.8238	1.2779
4	-0.3654	2.6730	-3.0381	9.5322	22.9398
5	-3.3778	1.8624	-1.3540	2.1771	46.4159

**Table 2.3** Coordinates of the Resulted Four-bar Linkage Joints in Their First Position

Joint	$A$	$B$	$P$	$C$	$D$
Coordinates	1.5630, 4.3296	1.7238, 1.0819	0.0120, -0.0305	-1.8743, 1.1612	-3.8165, 6.8238

**Figure 2.5** The four-bar linkage and the desired and generated motions.

When the other dyad was added to the structural error, as in Eq. (2.5), and the Grashof's condition and link length constraints were applied, the resulted linkage was the same as above. The optimized  $E_{Rmin}$  was 1.8521. The link length and Grashof's constraints were applied and the transmission angle requirement was also imposed but the acceptable range was expanded to  $25^\circ$  to  $155^\circ$ ; otherwise the resulted minimum of the structural error was too large.

#### **2.4.2 Continuous Path Generation**

The path to be synthesized is specified by 20 points with a cusp at the origin, as listed in Table 2.4. It is an arbitrary spline curve drawn in AutoCAD. Since the path starts at a cusp, the linkage's two side links,  $AB$  and  $CD$ , must point at the cusp at their first positions. This condition helps to choose the initial guess for the mechanism.

Given an initial guess of  $(5, 5)$ ,  $(3,3)$ ,  $(-1,4)$ , and  $(-2,8)$  for joint  $A$ ,  $B$ ,  $C$ , and  $D$ , respectively, the optimization process finds the optimal linkage, whose joint coordinates at their first position are listed in Table 2.5.



**Table 2.4** Desired and Generated Path Points

Point No.	Desired Path		Generated Path	
	$x$	$y$	$x$	$y$
1	0.0000	0.0000	0.0235	0.0417
2	0.4599	0.0000	0.5173	-0.0686
3	1.3311	-0.1259	1.3442	-0.1812
4	2.1263	-0.2173	2.1236	-0.2213
5	3.0007	-0.2669	3.0599	-0.2901
6	3.4921	-0.2827	3.5013	-0.2859
7	4.0926	-0.2632	4.1015	-0.2371
8	4.9115	-0.1501	4.8979	-0.1735
9	5.4371	-0.0706	5.3527	-0.2098
10	5.7692	-0.1450	5.8116	-0.1752
11	5.9300	-0.3603	5.9922	-0.3782
12	5.8298	-0.7703	5.8024	-0.7393
13	5.4794	-1.0504	5.4035	-1.0017
14	4.7572	-1.3449	4.6903	-1.2659
15	4.0139	-1.4121	4.0087	-1.3663
16	3.3049	-1.2991	3.3321	-1.1857
17	2.4233	-0.9376	2.4227	-0.9202
18	1.7184	-0.5327	1.8668	-0.5181
19	1.2056	-0.2386	1.3345	-0.1228
20	0.6334	-0.0407	0.7140	0.0739

**Table 2.5** Synthesized Four-bar Path Generation Linkage

Joint	$A$	$B$	$P$	$C$	$D$
Coordinates	4.5791, 2.0410	3.3129, 1.4766	0.0235, 0.0417	2.2581, 3.1304	4.2684, 5.9174

Figure 2.6 plots the linkage together with the desired and the generated paths. The generated path approximates the desired path closely. The total computing time is about 24 seconds and the minimized  $E_R = 5.7285$ . In this example, the link length, the Grashof's, and a loose transmission angle ( $30^\circ$  to  $150^\circ$ ) constraints are applied.

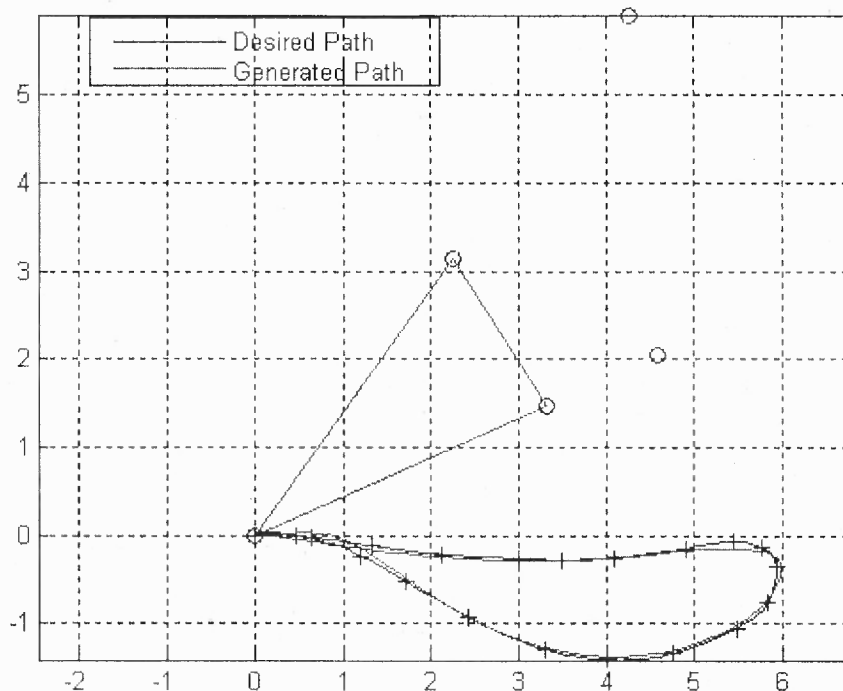


**Figure 2.6** The optimized linkage with the desired and the generated paths.

## 2.5 Conclusion

The idea of link length structural error is introduced and optimal synthesis model based on this compact structural error is established. This indirect structural error is proven to be equivalent to the conventional one for planar four-bar motion and path generation.

It can be expected that the synthesis method presented in this chapter has disadvantages. The two optimal dyads found by this method may not form the overall optimal four-bar linkage. And the absence of input crank angles in the design variables

adds difficulties to the order constraint.

Despite of these limitations, this method greatly simplifies the formulation of structural error and facilitates the optimization because it has a compact polynomial form of structural error whose explicit expressions of gradient vector and Hessian matrix are easily accessible. The synthesis examples clearly demonstrate the power of this approach in generating both optimal motions and paths.

The next chapters will focus on the application of the proposed method to the synthesis of adjustable mechanisms for multi-phase optimal motion, path, and function generation.

## CHAPTER 3

### OPTIMAL MULTI-PHASE MOTION GENERATION

#### 3.1 Introduction

As introduced in Chapter 1, multi-phase motion generation methods have been reported by many researchers. However, all these methods can only design linkages capable of achieving limited number of desired precision rigid body positions. For example, a planar four-bar linkage with the side-link length adjustable can guide its coupler through six prescribed positions. The positions are divided into two phases, each containing about three of them.

The industrial applications of motion generation usually need the moving body to pass through more given positions or impose additional requirements to the motion of the body between the given positions, while do not require it to pass through the positions exactly, because position errors of linkages can not be eliminated during manufacturing, assembly, and normal use. It is usually acceptable if the position error is within a reasonable range. There comes the concept of optimal motion generation.

With optimal motion generation, the mechanism is not designed to guide its coupler link through several prescribed precision rigid body positions but through a larger number of positions within an acceptable error. Using this approach, the adjustment to the mechanism allows the mechanism to achieve another series of many rigid body positions. Each phase of the adjustable mechanism contains theoretically unlimited number of positions, as long as the error is small enough to be acceptable. In synthesis practice, however, too many design positions are neither necessary nor practical – more positions

usually mean poorer solutions.

Introducing optimal synthesis approaches into design of adjustable mechanisms adds their versatility: although at the cost of less accuracy, the large number of additional positions provides more possibilities of controlling the generated motion.

### 3.2 Adjustable Dyad for Optimal Motion Generation

In Chapter 2, the synthesis model for an optimal motion generation dyad is established. To make it adjustable, three options are available: adjusting the link length, the moving pivot, or the fixed pivot.

#### 3.2.1 Three Types of Adjustments

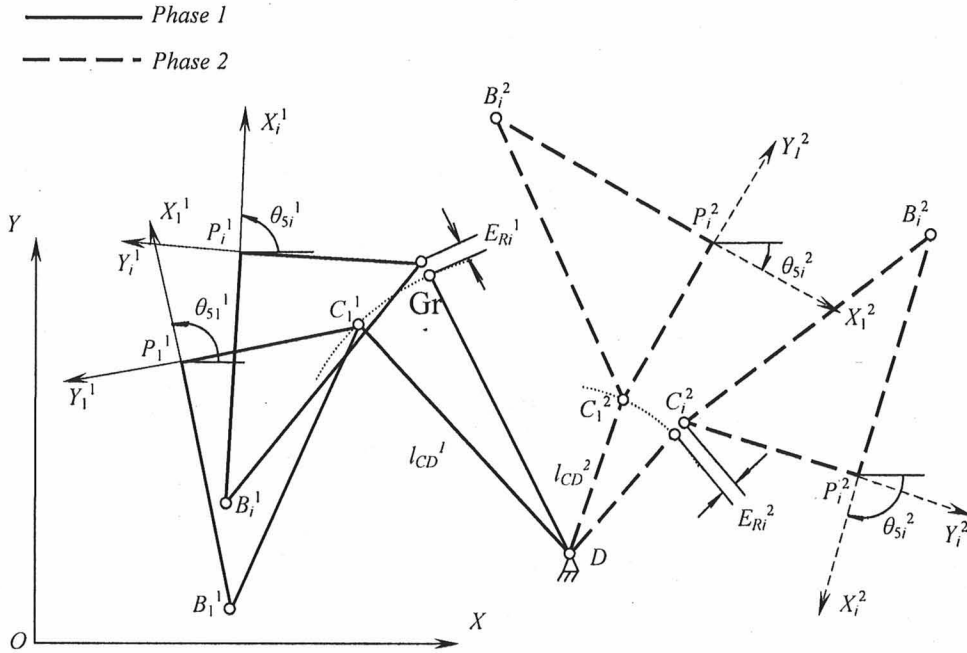
##### a. Adjustable Link Length

Figure 2.1 is redrawn below as Figure 3.1 with an additional phase shown in dashed lines. The two phases share every dimension except a different link length of  $CD$ . For motion generation, the coupler points  $P_i^1(x_i^1, y_i^1)$  and  $P_i^2(x_i^2, y_i^2)$  and coupler angles  $\theta_{Si}^1$  and  $\theta_{Si}^2$  are given. For phase 1, the link length structural error is

$$E_R^1 = \sum_{i=2}^n \eta_i^1 [(C_i^1 - D)^T (C_i^1 - D) - (C_1^1 - D)^T (C_1^1 - D)]^2 \quad (3.1)$$

where  $\eta_i$  is a weighting coefficient for each design points; the unknowns are

$$C_1^1 = (x_{C1}^1, y_{C1}^1)^T, \quad D = (x_D, y_D)^T, \quad (3.2)$$



**Figure 3.1** An optimal dyad with adjustable link length for motion generation.

Coordinates of joint  $C$  at design positions  $C_i$  ( $i=2,3,\dots,n$ ) can be obtained by

$$C_i^1 = (x_{C_i}^1, y_{C_i}^1)^T, \quad (x_{C_i}^1, y_{C_i}^1, 1)^T = T_{1i}^1 (x_{C_1}^1, y_{C_1}^1, 1)^T \quad (3.3)$$

where  $i=2, 3, 4, \dots, n$ ,  $T_{1i}^1$  is the coordinate transformation matrix from frame  $X_1^1 P_1^1 Y_1^1$  to frame  $X_i^1 P_i^1 Y_i^1$ ,

$$T_{1i}^1 = \begin{bmatrix} \cos(\theta_{s_i}^1 - \theta_{s_1}^1) & -\sin(\theta_{s_i}^1 - \theta_{s_1}^1) & -\cos(\theta_{s_i}^1 - \theta_{s_1}^1)x_1^1 + \sin(\theta_{s_i}^1 - \theta_{s_1}^1)y_1^1 + x_i^1 \\ \sin(\theta_{s_i}^1 - \theta_{s_1}^1) & \cos(\theta_{s_i}^1 - \theta_{s_1}^1) & -\sin(\theta_{s_i}^1 - \theta_{s_1}^1)x_1^1 - \cos(\theta_{s_i}^1 - \theta_{s_1}^1)y_1^1 + y_i^1 \\ 0 & 0 & 1 \end{bmatrix} \quad (3.4)$$

For phase 2, a similar link length structural error can be obtained as

$$E_R^2 = \sum_{i=1}^n \eta_i^2 [(C_i^2 - D)^T (C_i^2 - D) - (C_1^2 - D)^T (C_1^2 - D)]^2 \quad (3.5)$$

Here the unknowns are still  $C_1^1$  and  $D$  as in Eq. (3.2). Coordinates of joint  $C$  in phase 2,  $C_i^2$ , ( $i=1, 2, \dots, n$ , suppose phase 2 also has  $n$  prescribed positions) can be obtained by

$$C_i^2 = (x_{Ci}^2, y_{Ci}^2)^T, \quad (x_{Ci}^2, y_{Ci}^2, 1)^T = T_{1i}^2 (x_{C1}^1, y_{C1}^1, 1)^T \quad (3.6)$$

$T_{1i}^2$  ( $i=1, 2, \dots, n$ ) is the coordinate transformation matrix from frame  $X_1^1 P_1^1 Y_1^1$  (the first position of phase 1) to frame  $X_i^2 P_i^2 Y_i^2$  (the  $i^{\text{th}}$  position of phase 2):

$$T_{1i}^2 = \begin{bmatrix} \cos(\theta_{5i}^2 - \theta_{51}^1) & -\sin(\theta_{5i}^2 - \theta_{51}^1) & -\cos(\theta_{5i}^2 - \theta_{51}^1)x_1^1 + \sin(\theta_{5i}^2 - \theta_{51}^1)y_1^1 + x_i^2 \\ \sin(\theta_{5i}^2 - \theta_{51}^1) & \cos(\theta_{5i}^2 - \theta_{51}^1) & -\sin(\theta_{5i}^2 - \theta_{51}^1)x_1^1 - \cos(\theta_{5i}^2 - \theta_{51}^1)y_1^1 + y_i^2 \\ 0 & 0 & 1 \end{bmatrix} \quad (3.7)$$

The overall structural error

$$E_R = E_R^1 + E_R^2 = \sum_{i=2}^n \eta_i^1 [(C_i^1 - D)^T (C_i^1 - D) - (C_1^1 - D)^T (C_1^1 - D)]^2 + \sum_{i=2}^n \eta_i^2 [(C_i^2 - D)^T (C_i^2 - D) - (C_1^2 - D)^T (C_1^2 - D)]^2 \quad (3.8)$$

Minimizing  $E_R$  will give the optimal adjustable dyad that needs the least overall side-link length change to guide its coupler through desired positions in both phases.

Notice that the adjustable link length of the side-link does not show as a design variable in the structural error at all. The optimization finds the best circle point  $C$  and center point  $D$ , hence determines the link lengths in both phases.

b. *Adjustable Moving Pivot*

If the moving pivot is made adjustable, the design variables become

$$C_1^1 = (x_{C_1^1}, y_{C_1^1})^T, C_1^2 = (x_{C_1^2}, y_{C_1^2})^T, D = (x_D, y_D)^T, \quad (3.9)$$

Phase 1 is the same as in link length adjustment problem. For phase 2, the coordinates of joint  $C$  can be obtained by

$$C_i^2 = (x_{C_i^2}, y_{C_i^2})^T, (x_{C_i^2}, y_{C_i^2}, 1)^T = T_{1i}^2 (x_{C_1^2}, y_{C_1^2}, 1)^T \quad (3.10)$$

$C_i^2$  here is obtained from  $C_1^2$ , other than from  $C_1^2$  as in link length adjustment.  $T_{1i}^2$  ( $i=2, 3, \dots, n$ ) is the coordinate transformation matrix from frame  $X_1^2 P_1^2 Y_1^2$  to frame  $X_i^2 P_i^2 Y_i^2$ ,

$$T_{1i}^2 = \begin{bmatrix} \cos(\theta_{5i}^2 - \theta_{51}^2) & -\sin(\theta_{5i}^2 - \theta_{51}^2) & -\cos(\theta_{5i}^2 - \theta_{51}^2)x_1^2 + \sin(\theta_{5i}^2 - \theta_{51}^2)y_1^2 + x_i^2 \\ \sin(\theta_{5i}^2 - \theta_{51}^2) & \cos(\theta_{5i}^2 - \theta_{51}^2) & -\sin(\theta_{5i}^2 - \theta_{51}^2)x_1^2 - \cos(\theta_{5i}^2 - \theta_{51}^2)y_1^2 + y_i^2 \\ 0 & 0 & 1 \end{bmatrix} \quad (3.11)$$



The link length structural error for both phases can be given by

$$E_R = E_R^1 + E_R^2 = \sum_{i=2}^n \eta_i^1 [(C_i^1 - D)^T (C_i^1 - D) - (C_1^1 - D)^T (C_1^1 - D)]^2 + \sum_{i=1}^n \eta_i^2 [(C_i^2 - D)^T (C_i^2 - D) - (C_1^1 - D)^T (C_1^1 - D)]^2 \quad (3.12)$$

Notice that link lengths in both phases are compared with their own first position.

### c. Adjustable Fixed Pivot

Similar to adjustable moving pivot, the unknowns now are

$$C_1^1 = (x_{C1}^1, y_{C1}^1)^T, D^1 = (x_D^1, y_D^1)^T, D^2 = (x_D^2, y_D^2)^T \quad (3.13)$$

$C_i^1$  and  $C_i^2$  are the same as in 3.2.1, and the link length structural error for both phases can be given by

$$E_R = E_R^1 + E_R^2 = \sum_{i=2}^n \eta_i^1 [(C_i^1 - D^1)^T (C_i^1 - D^1) - (C_1^1 - D^1)^T (C_1^1 - D^1)]^2 + \sum_{i=1}^n \eta_i^2 [(C_i^2 - D^2)^T (C_i^2 - D^2) - (C_1^1 - D^2)^T (C_1^1 - D^2)]^2 \quad (3.14)$$

### 3.2.2 Combination of Adjustments

Though not often, combination of several types of adjustments are sometimes used to provide more flexibility and capability of the mechanisms in exact synthesis. In optimal multi-phase motion generation, multiple adjustments are not needed as much. However, in

cases when the desired phases of motions are so diversified that linkages with one kind of adjustment are not able to generate the motions satisfyingly, the combination of adjustments may be required.

The combination of adjustments can be easily handled using the link length structural error based optimal synthesis method by simply combining the formulations of the three types of adjustments. The resulted structural error can be slightly different with several additional design variables. For example, if both the fixed and the moving pivots are adjustable, the design variables are

$$C_1^1 = (x_{C_1^1}, y_{C_1^1})^T, C_1^2 = (x_{C_1^2}, y_{C_1^2})^T, D^1 = (x_D^1, y_D^1)^T, D^2 = (x_D^2, y_D^2)^T \quad (3.15)$$

And the structural error is the same as in adjustable moving pivot problem except for the added variable  $D^2$ :

$$E_R = E_R^1 + E_R^2 = \sum_{i=2}^n \eta_i^1 [(C_i^1 - D^1)^T (C_i^1 - D^1) - (C_1^1 - D^1)^T (C_1^1 - D^1)]^2 + \sum_{i=1}^n \eta_i^2 [(C_i^2 - D^2)^T (C_i^2 - D^2) - (C_1^1 - D^1)^T (C_1^1 - D^1)]^2 \quad (3.16)$$

### 3.2.3 More Phases

The proposed synthesis method also applies to three or more phase mechanisms. By simply adding another term to the structural error and some additional constraints for each additional phase, the synthesis procedure remains the same.

### 3.3 Optimal Synthesis of the Four-bar Linkage

Due to the input motion, it is difficult to adjust the driving-side fixed pivot (the shaft where the input actuator is connected) and the link length (usually fully rotating about both the ground frame and the coupler) of a four-bar linkage. The only parameter left to adjust for the driving dyad is its moving pivot, while all parameters of the driven dyad are available for adjusting.

Even though it is possible that we achieve two phases of rigid body positions by only adjusting the driven dyad while leaving the driving dyad unchanged, it is not recommended because when the two phases of motion are apparently distinct, using the same dyad to generate both of them may result in large error in both phases. Therefore the adjustment to the moving pivot of the driving dyad is always recommended. Adjustment to the other dyad can be arbitrary among the three.

As discussed in Chapter 2, the synthesis of the other dyad can be accomplished by either finding several local minimum of the structural error for a single adjustable dyad or by combining the two dyads errors into one.

#### 3.3.1 The Two Dyads Combined

As an example, we give the combined link length structural error for adjustable driving and driven side-links moving pivot problem, as shown in Fig. 3.2. These adjustments can be easily realized by actuators mounted onto the moving coupler and controlling and powering wires connected to the ground frame through the driven side link.

There are totally six vector unknowns:

$$\begin{aligned} B_1^1 &= (x_{B_1^1}, y_{B_1^1})^T, B_1^2 = (x_{B_1^2}, y_{B_1^2})^T, A = (x_A, y_A)^T, \\ C_1^1 &= (x_{C_1^1}, y_{C_1^1})^T, C_1^2 = (x_{C_1^2}, y_{C_1^2})^T, D = (x_D, y_D)^T \end{aligned} \quad (3.17)$$

Each dyad yields a structural error as given in 3.3.2. The combined structural error for both dyads can be given by

$$\begin{aligned} E_R &= E_R^1 + E_R^2 \\ &= \sum_{i=2}^n \{ \eta_i^1 [(C_i^1 - D)^T (C_i^1 - D) - (C_i^1 - D)^T (C_i^1 - D)]^2 + \mu_i^1 [(B_i^1 - A)^T (B_i^1 - A) - (B_i^1 - A)^T (B_i^1 - A)]^2 \} \\ &\quad + \sum_{i=1}^n \{ \eta_i^2 [(C_i^2 - D)^T (C_i^2 - D) - (C_i^2 - D)^T (C_i^2 - D)]^2 + \mu_i^2 [(B_i^2 - A)^T (B_i^2 - A) - (B_i^2 - A)^T (B_i^2 - A)]^2 \} \end{aligned} \quad (3.18)$$

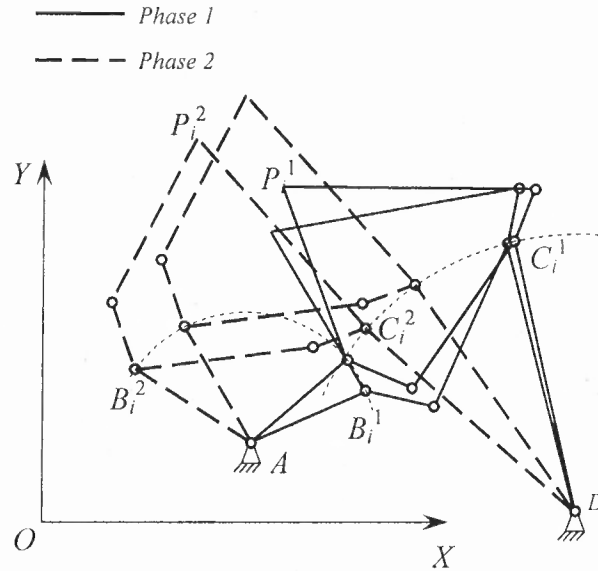


**Figure 3.2** Adjustable moving pivots for both dyads.

### 3.3.2 Constraints

The optimal synthesis problem becomes:

Minimize  $E_R$

Subject to the following constraints:

#### a. Grashof's criteria

Suppose link AB is to be the input crank, then it is preferred to be the shortest link of because a crank-rocker is usually desired. The longest link is not determined yet, thus a general form of Grashof's condition can be given as  $AB + r_l < r_p + r_q$  for both phases.

#### b. Transmission angle

The transmission angle  $\mu$  ( $\angle BCD$ ) can be easily calculated for both phases. The transmission angle is limited to  $\mu_{\min} < \mu < \mu_{\max}$ .

#### c. Link lengths

At least one link length constraints has to be imposed to this problem to identify the two adjustable dyads. It can be implemented by constrain the link length  $AD$  to be larger than a small value. Other constraints can be applied by restricting joint coordinates in acceptable ranges as needed.

#### d. Order Constraint

Order requirement is associated with the input crank angle at all design positions. The input angle can be obtained by

$$\theta_{li} = \tan^{-1} \left( \frac{y_{Bi} - y_C}{x_{Bi} - x_C} \right), \quad -\pi/2 < \theta_{li} < \pi/2 \quad (3.19)$$

For  $\theta_{1i}$  out of this range, add  $\pi$  to it. The order constraints can be then applied as

$$\theta_{1i} - \theta_{1(i+1)} < 0 \text{ or } \theta_{1i} - \theta_{1(i+1)} > 0, i=1,2,\dots,n, \quad (3.20)$$

### 3.4 Continuously Adjustable Mechanisms

Another advantage of this synthesis method is its ability to exactly generate the desired motion at all chosen positions with the assistance of a continuously adjustable (or in other words, real-timely controllable) side links. Once the optimal synthesis of an adjustable mechanism is completed using the above technique, the side-link length changes have been obtained. These changes are minimized at all design points and are supposed to be small. If an adjusting device is mounted on this link and is made to real-timely adjust the length of the side-link at the amount of the calculated link length changes, the optimal linkage can then generate the given rigid body positions precisely at all design positions. This continuous adjustment can be realized either by an actuator or a cam. Distinct from other optimal synthesis methods, the proposed technique finds the required link length changes directly as the result of the optimization process.

To generate the desired rigid body positions precisely, the required continuous side-link length adjustment for phase 1 at position  $i$  is

$$L_{Ri}^1 = [(C_i^1 - D)^T (C_i^1 - D)]^{1/2} - [(C_1^1 - D)^T (C_1^1 - D)]^{1/2} \quad (3.21)$$

where  $i=2,3,\dots,n$ . The adjustment amount for phase 2 is similar to Eq. (3.19).

With continuously adjustable side links, the linkage designed under this method seems to have two “modes”: when the two side-link lengths are fixed at their optimal values in each phase, which are their lengths at the first position, the linkage guides its coupler link through the desired positions optimally; when the side-link lengths are continuously adjusted at the amount given by Eq. (3.19), the adjustable linkage can generate the desired rigid body positions precisely. This capability provides more flexibility for the adjustable mechanisms.

### 3.5 Synthesis Example

Two phase of rigid body positions (23 positions each, as listed in Table 3.1) were to be synthesized by an adjustable four-bar linkage. These positions are required by a grab which feeds material to two different conveyers, as demonstrated in Figure 3.3. Certain paths need to be followed for the grab to clear other equipments, as well as angular positions have to be maintained while loading, discharging, and transportation.

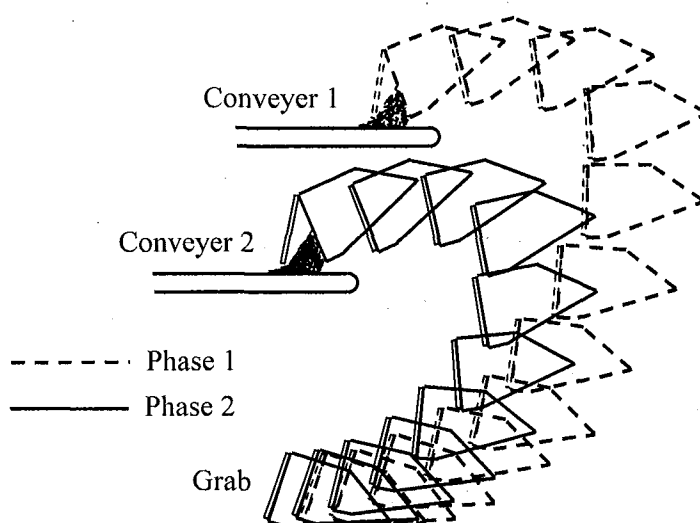


**Figure 3.3** A grab feeding material to two conveyers.

**Table 3.1** Desired Two Phases of Rigid Body Positions

Position No.	Desired Motion 1			Desired Motion 2		
	$x$	$y$	$\theta$	$x$	$y$	$\theta$
1	-0.04914	-0.02085	0.37	0.1243311	0.012769	0.55
2	0.319725	-0.04012	2.36	0.4824177	0.111173	0.78
3	0.70659	-0.00113	3.94	0.8286765	0.246208	0.63
4	1.097916	0.095576	5.09	1.1554199	0.412565	0.06
5	1.480917	0.246568	5.78	1.4562103	0.603565	0.97
6	1.844081	0.445294	5.95	1.72607	0.811745	2.51
7	2.177677	0.682262	5.47	1.9615554	1.029659	4.58
8	2.474235	0.945843	4.25	2.1606404	1.250656	7.18
9	2.728781	1.223945	2.17	2.3224113	1.469393	10.29
10	2.938567	1.506237	0.81	2.4466711	1.681886	13.84
11	3.102275	1.785631	4.63	2.5335871	1.885143	17.77
12	3.219157	2.057949	9.15	2.5834736	2.076634	21.97
13	3.288606	2.320278	14.21	2.5967127	2.253822	26.36
14	3.310211	2.569388	19.61	2.57376	2.413875	30.83
15	3.284034	2.800978	25.19	2.5151719	2.553567	35.31
16	3.210836	3.009615	30.82	2.4216081	2.669305	39.68
17	3.092189	3.189017	36.34	2.293786	2.75723	43.86
18	2.930424	3.332415	41.65	2.1323744	2.813375	47.74
19	2.728467	3.432902	46.59	1.9378303	2.833868	51.21
20	2.489544	3.483768	51.00	1.7101956	2.815219	54.11
21	2.216783	3.478855	54.70	1.448912	2.754754	56.31
22	1.912765	3.41309	57.46	1.1527879	2.651291	57.61
23	1.579175	3.283389	59.03	0.8203974	2.506147	57.84

**Table 3.2** Optimized Adjustable Linkage

Joint	$A$	$B^1$	$C^1$	$D$	$P$	$B^2$	$C^2$
$x$	2.5813	1.7251	-2.4784	-3.1165	0.0132	2.9523	-2.0363
$y$	3.2926	1.0808	1.0135	5.9238	0.0254	0.9501	1.0915



Both moving pivots were adjustable. The Grashof's, transmission angle, and link length constraints were applied. The optimal adjustable linkage found is listed in Table 3.2. Table 3.3 shows the generated motions. Figure 3.4 plots the generated mechanism together with the desired and the generated motions. The two motions appear close to each other.

**Table 3.3** Generated Motions

Position No.	Generated Motion 1			Generated Motion 2		
	$x$	$y$	$\theta$	$x$	$y$	$\theta$
1	7.86E-05	9.92E-06	1.68E-05	-2.70E-06	1.40E-05	0.000452
2	0.351665	-0.03879	2.499542	0.3602485	0.09197	0.098035
3	0.727247	-0.01793	4.588842	0.7086674	0.220176	0.177891
4	1.112881	0.063292	6.274666	1.0376233	0.379567	0.860379
5	1.495275	0.202667	7.533538	1.3407095	0.563772	1.985567
6	1.862236	0.3947	8.302738	1.61293	0.765673	3.586329
7	2.203205	0.630417	8.47167	1.8507661	0.978122	5.683073
8	2.509884	0.897596	7.881504	2.0520707	1.19462	8.275044
9	2.776721	1.182143	6.353163	2.2158003	1.40977	11.33537
10	3.000833	1.471123	3.75968	2.3416596	1.619355	14.81192
11	3.181015	1.756017	0.10817	2.4297743	1.820065	18.63308
12	3.316426	2.033258	4.447804	2.4804683	2.009068	22.71551
13	3.405939	2.301685	9.676544	2.4941604	2.183614	26.97072
14	3.448341	2.559707	15.34478	2.4713397	2.340761	31.30878
15	3.442867	2.803986	21.25396	2.412568	2.477266	35.63928
16	3.389601	3.029423	27.24203	2.3184655	2.589594	39.86984
17	3.289646	3.229643	33.17132	2.1896548	2.674002	43.90319
18	3.145124	3.397535	38.91431	2.0266499	2.726684	47.63323
19	2.959028	3.525694	44.34058	1.8296936	2.743982	50.94055
20	2.734971	3.606781	49.30492	1.5985633	2.722689	53.68826
21	2.476814	3.633828	53.63606	1.3324134	2.66051	55.7192
22	2.188202	3.600623	57.12656	1.0298034	2.556777	56.85758
23	1.872071	3.502317	59.52708	0.6892129	2.41347	56.91969

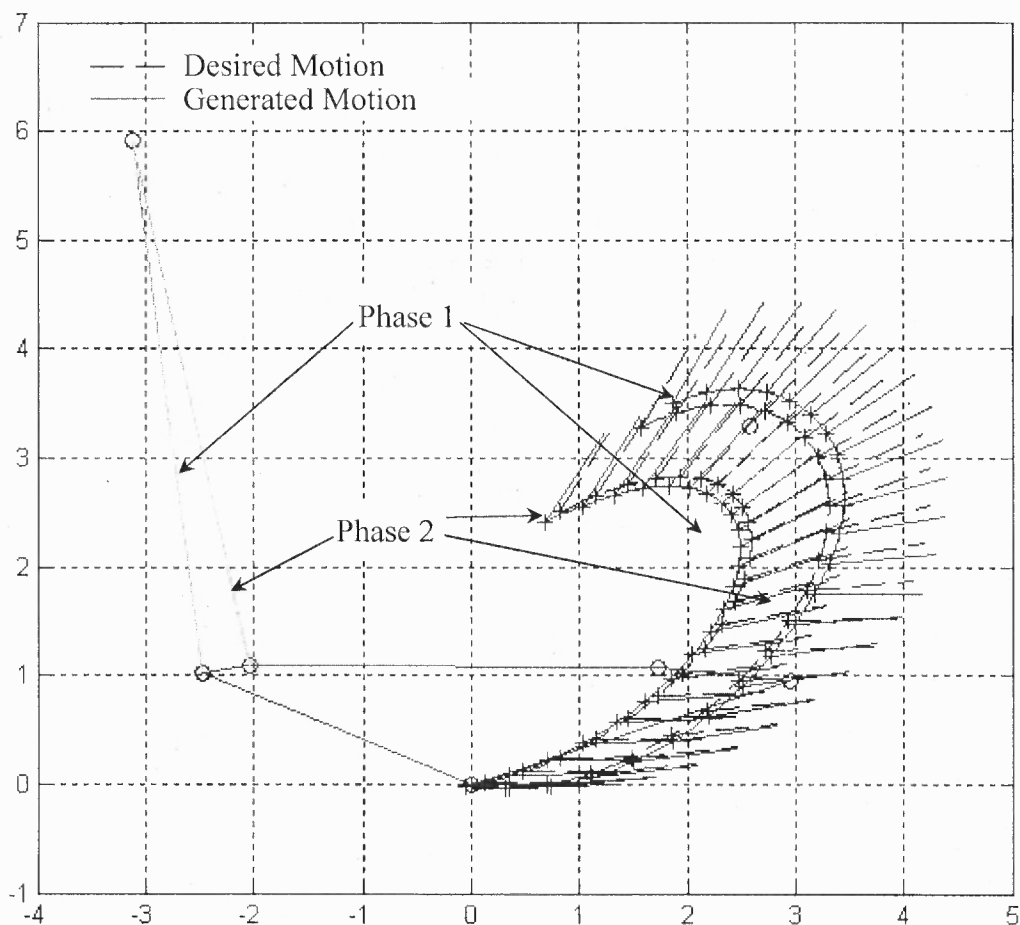


**Figure 3.4** The optimized adjustable linkage and the motions.

### 3.6 Conclusion

In this chapter, the optimal synthesis method developed in Chapter 2 is applied to the synthesis of adjustable motion generating four-bar linkages. The adjustable optimal dyad is first modeled and the link length structural error for two phase problems was established. The technique to combine the two optimal dyads into a four-bar linkage is then presented. A numerical example is given to verify the method. With the assistance of continuously adjustable side links, the linkage can also generate the desired rigid body positions precisely.

## CHAPTER 4

### OPTIMAL MULTI-PHASE PATH GENERATION

#### 4.1 Introduction

There are two types of path generation tasks: point-to-point path generation and continuous path generation. *Point-to-point* path generation specifies only a few precision points on the desired path and requires the designed mechanism to guide its coupler point through these precision points exactly. For a four-bar linkage, since there are only nine independent design variables, the maximum number of precision points is nine.

On the other hand, *continuous* path generation specify the whole path or many points on the path. Since it is impractical to generate an absolutely precise whole path as we desire, optimal synthesis methods are used to synthesize linkages for continuous path generation. The objective function, called structural error, is conventionally formulated as the sum of the square distance between the desired and the generated paths over a number of comparison points.

Many effective synthesis methods have been developed for adjustable point-to-point path generation [18-22]. As for adjustable continuous path generation, the only work reported is done by Zhou and Ting [39]. In this work, they adjusted the position of a slider-crank linkage's slider guider (the slider offset value) to generate a set of elliptical paths which have the same short axis. They also introduced the position structural error of the slider guider, which can effectively reflect the overall error between the generated and desired paths while avoiding the selection of comparison points. The synthesis model is optimized using a genetic algorithm. However, this method is not

effective for generating a set of arbitrary paths other than some co-short-axis ellipses. The evaluation of the structural error requires calculation of driving dyad link lengths using the longest and shortest distances from the fixed pivot to desired paths. For arbitrarily given paths, any position of driving crank fixed pivot will result in different driving dyad link lengths for different phases, making the procedure not applicable.

In this chapter, an optimal synthesis method for adjustable four-bar mechanisms generating multiple arbitrary continuous paths is presented. The designed linkage with one adjustment is able to approximately guide its coupler point through two arbitrarily given paths specified by a number of points. A numerical example is given to verify the method.

## 4.2 Multiple Continuous Path Generation Problem

An adjustable planar four-bar linkage is to be designed to guide a coupler point through path 1 in phase 1 and through path 2 in phase 2, as shown in Fig. 4.1. Link  $AB$  is chosen to be the input crank, which needs to achieve a full rotation. The adjustment can be made to the fixed pivot, moving pivot, or the link length of the driven dyad or the moving pivot of the driving dyad. The fixed pivot and the link length of the driving dyad are not recommended for adjustment because they are associated with the input motion – the fixed pivot is where the input axis lies, and the crank has to fully rotate about both the ground frame and the coupler.

The two paths to be synthesized are arbitrarily-chosen continuous closed curves given by specifying  $n$  target points on each of them (a typical  $n$  lies between 10 and 30). The linkage is required to guide its coupler point through these points as close as possible. Considering the great number of specified points on each path, trajectories between these

points are not specified and the path is still considered continuous.

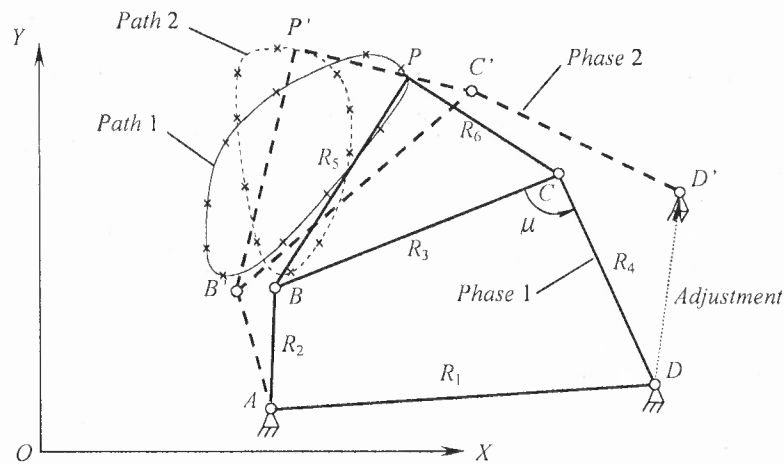


**Figure 4.1** The desired paths and a sample adjustable linkage.

Instead of giving one or two additional precision points, the adjustment in this case makes the linkage capable of tracing an entire continuous path in each phase. Solving this problem will greatly extend the ability of adjustable mechanisms and make them more competitive with multi-DOF robots in generating multiple continuous paths.

Although this particular problem is restricted to one adjustment and two phases, the developed synthesis technique could be applied to other types of adjustments and more phases.

### 4.3 Optimal Multiple Path Generation: Adjustable Driven Dyad

The driven dyad is preferred for adjustments for its independence from the input. Conventional optimal synthesis method can be improved to apply to this task. However, considering the great number of design variables (11 linkage dimensions and  $2n$  input crank angles) and highly nonlinear error function, the computation could be much time

consuming. Also, no reported optimal synthesis technique can treat the adjustment well. There is a need to develop a new synthesis procedure.

A close look at this adjustable linkage reveals that the driving dyad remains the same for both phases. Since the driving crank is to be fully rotatable in both phases, these are the additional requirements which can be used to determine the driving dyad. The driven dyad can be found later.

### 4.3.1 Synthesis of the Driving Dyad

As in Figure 4.2, for point  $P$  of the dyad  $ABP$  to trace a given path, the following conditions must be satisfied:

$$R_2 + R_5 = R_{\max} \quad (4.1)$$

$$|R_2 - R_5| = R_{\min} \quad (4.2)$$

$R_2$  and  $R_5$  are the lengths of the driving link  $AB$  and coupler link  $BP$ .  $R_{\max}$  and  $R_{\min}$  are the longest and shortest distances from the center point  $A$  to the desired path.  $R_{\max}$  or  $R_{\min}$  exists at the extreme configuration of the dyad, which can be called “stretched” or “folded”, as shown in Figure 4.2.

To achieve full rotation of the input link  $AB$  about the ground link  $AD$ , Grashof’s criterion requires the mechanism to be a crank-rocker or a double-crank, and a crank-rocker is usually preferred, thus  $AB$  is the shortest link. The sign of  $R_2 - R_5$  depends on the joint  $A$  lying inside or outside of the path loop: if inside,  $R_2 > R_5$ , and outside,  $R_2 < R_5$ ; otherwise the link  $AB$  is unable to finish a full turn.

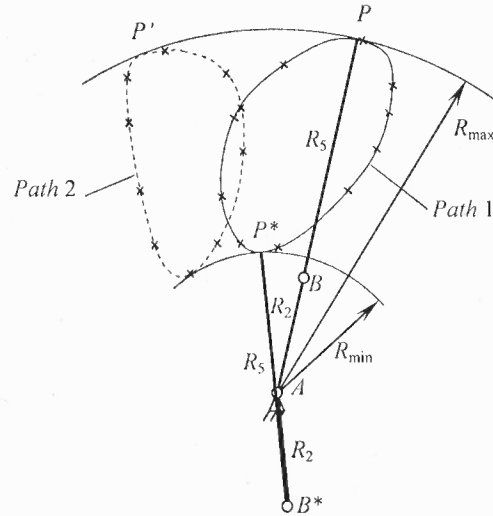


**Figure 4.2**  $R_{\max}$  and  $R_{\min}$  of the driving dyad.

$R_2$  and  $R_5$  remain the same for both phases, so do  $R_{\max}$  and  $R_{\min}$ ,

$$R_{\max}^1 = R_{\max}^2 \quad (4.3)$$

$$R_{\min}^1 = R_{\min}^2 \quad (4.4)$$

Conditions (4.3) and (4.4) can be used to find coordinates of the proper center point  $A$ . Qualified center point holds the same longest and shortest distances to both paths. Existence of center point  $A$  depends on topological structure of the desired paths. In some cases (for example, when one path is totally enclosed by the other with no intersection between the two), it may be impossible to find a suitable center point, and therefore the paths are not synthesizable with given hardware. In this work, we only consider the situation under which a suitable center point can be found. This generally requires both paths to lie tangentially between two concentric circles with only one tangent point with each circle.

In order to measure distances from the possible center point  $A$  to the paths more precisely, the curves are refined by spline interpolation, which gives more imaginary points between the specified ones. Suitable number of refined points depends on accuracy required and acceptable computing time. Typically 100 to 200 points can be easily handled by an average PC in the following optimization process.  $R_{\max}$  and  $R_{\min}$  can be then chosen from distances calculated from the center point to all the refined points. The best center point is found by an optimization process that minimizes the errors of Eq. (4.3) and Eq. (4.4) at these refined points.

To find the best center point  $A(x_A, y_A)$ , the following error function is to be minimized:

$$E_A = \left( \left[ (x_A - x_i^1)^2 + (y_A - y_i^1)^2 \right]_{\max}^{1/2} - \left[ (x_A - x_i^2)^2 + (y_A - y_i^2)^2 \right]_{\max}^{1/2} \right)^2 + \left( \left[ (x_A - x_i^1)^2 + (y_A - y_i^1)^2 \right]_{\min}^{1/2} - \left[ (x_A - x_i^2)^2 + (y_A - y_i^2)^2 \right]_{\min}^{1/2} \right)^2, \quad i=1,2,\dots,n \quad (4.5)$$

where  $P_i^1(x_i^1, y_i^1)$  and  $P_i^2(x_i^2, y_i^2)$  desired path points in phase one and phase two, respectively, and  $n$  is the number of points on each path. All coordinates are given with respect to the global coordinate system  $XOY$  which is fixed on the ground. Once  $A(x_A, y_A)$ ,  $R_{\max}$  and  $R_{\min}$  are found by the optimization, link lengths  $R_2$  and  $R_5$  can be determined from Eq. (4.1) and (4.2).

One of the constraints needed is to restrict  $(x_A, y_A)$  in a suitable range so that the resulted lengths of  $R_2$  and  $R_5$  are acceptable. As mentioned above, joint  $A$  has to stay either inside or outside of both path loops, otherwise the resulted link  $AB$  is not able to achieve a full turn. This can be accomplished by kicking the troublesome regions out of the design



space. Those regions are the area that is enclosed by one path but excluded by the other one.

The order constraints may also be imposed by restricting  $\theta_{2i}$  as following:

$$\theta_{2i+1} - \theta_{2i} > 0, i = 1, 2, \dots, n \quad (4.6)$$

where as in Figure 4.3,

$$\theta_{2i} = \alpha_i \pm \gamma_i = \arg(\overrightarrow{AP_i}) \pm \cos^{-1} \left( \frac{R_2^2 + R_{P_i}^2 - R_5^2}{2R_2 R_{P_i}} \right), 0 \leq \gamma_i \leq \pi, i = 1, 2, \dots, n \quad (4.7)$$

### 4.3.2 Determining the Coupler Angles

Once the input dyad is obtained, coupler angles at all design points of each phase can be calculated. For convenience, coupler angles  $\theta_{5i}$  are measured from  $X$  axis of the fixed coordinate system  $XOY$  to the direction of link  $BP$  (not to the link  $BC$  because joint  $C$  is not known yet). At the point that gives  $R_{\max}$  or  $R_{\min}$ , there is only one configuration of the dyad, either stretched or folded. For all other design points, there exist two configurations of link  $AB$  and  $BP$ , as shown in Figure 4.3, in which the dyad lies on different side of the line  $AP$ , giving two different coupler angles. The couple angle are found by

$$\theta_{5i} = \alpha_i \mp \beta_i = \arg(\overrightarrow{AP_i}) \mp \cos^{-1} \left( \frac{R_5^2 + R_{P_i}^2 - R_2^2}{2R_5 R_{P_i}} \right), 0 \leq \beta_i \leq \pi, i = 1, 2, \dots, n \quad (4.8)$$

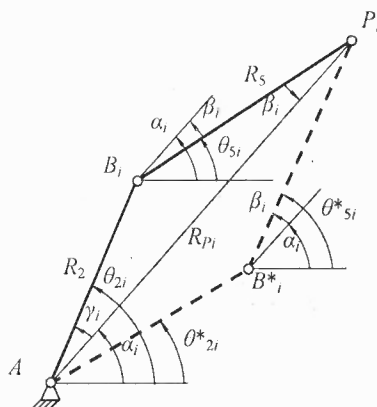


**Figure 4.3** The crank and coupler angles.

$\gamma_i$  in Eq. (4.7) and  $\beta_i$  in Eq. (4.8) have opposite signs and must be chosen in a way that when coupler point  $P$  passes through all design points once in sequence, driving crank finish a full unidirectional rotation. The following procedure is used to ease the sign choosing: Notice that these signs depend on which side of line  $AP$  the dyad lies on. In a full turn of input crank, the dyad can only pass line  $AP$  once at each of its two extreme configurations, which are achieved at the points that gives  $R_{\max}$  and  $R_{\min}$ , respectively. These two points divide the desired path into two pieces. The dyad remains on one side of line  $AP$  when  $P$  is moving on one piece and on the other side of  $AP$  for  $P$  on the other piece. Therefore,  $\beta_i$  in Eq. (7) contains the same sign for all design points on one piece, but opposite sign for points on the other. Following this rule, each phase has two sets of coupler angles, each corresponding to a different input crank rotation direction (clockwise or counterclockwise) for the same coupler point tracing direction. If the preferred input and path tracing directions are given to each phase, only one set of coupler angles can be chosen.

### 4.3.3 Optimal Synthesis of the Adjustable Driven Dyad

Adjustment to the position of the driven side-link fixed pivot  $D$  is the most desired because it is the easiest to adjust – it is placed on the fixed ground link and is not associated with input motion. The moving pivot and the link length are also adjustable.

Given desired path points  $P_i^1$  and calculated coupler angles  $\theta_{5i}^1$  (and  $P_i^2$  and  $\theta_{5i}^2$  in phase 2), the synthesis of the other dyad  $PCD^1$  and  $PCD^2$  becomes a multi-phase optimal motion generation problem. The objective now is to find an optimal dyad that guides the coupler through the given two phases of rigid body positions approximately, exactly as has been discussed in Section 3.2. Under the method developed in Chapter 3, the formulated structural error function for each kind of adjustment to the driven dyad is the same as in Section 3.2, thus not repeated here.

The constraints applied to the optimal synthesis of the driven dyad include:

#### 1. *Grashof's criteria*

Link AB is always the shortest link of this crank-rocker. With the driven fixed pivot adjustable, the length of ground link changes. A general form can be given as

$$r_2 + r_1 < r_p + r_q.$$

#### 2. *Transmission angle*

Given coordinates of pivots  $B$ ,  $C$  and  $D$ , the transmission angle  $\mu$  ( $\angle BCD$  as in Fig. 4.1) can be easily calculated. The transmission angle is limited to  $\mu_{\min} < \mu < \mu_{\max}$  for both phases.

#### 3. *Link lengths*

Link length constraints can be applied by restricting joint coordinates in acceptable ranges. If needed, they can also be directly constrained.

Order constraints have been imposed to the synthesis of the driving dyad. The driven dyad does not affect the input crank order.

The structural error  $E_R$  formulated in the proposed synthesis method is a fourth order polynomial of only six scalar unknowns for the adjustable driven moving or fixed pivot problem ( $x_{C1}$ ,  $y_{C1}$ ,  $x_D$ ,  $y_D$ ,  $x_D^1$ , and  $y_D^1$ ) or five for adjustable link length, much simpler than conventional structural error that would have  $(2n+6)$  unknowns in this case. Due to the small number of design variables, simple constraints, and less complicated structural error function, conventional gradient-based optimization methods in commercial software like Matlab® or Mathematica® can solve this problem well.

This method is also capable of three or more phase path generation, which simply adds some terms to the error function. With minor modification it can also handle other types of adjustment to the driven dyad such as the adjustment of the link length or the moving pivot.

#### **4.3.4 Continuous Adjustment**

Similar to Section 3.4, the optimal path generation mechanisms design with this method can also be made continuously adjustable to generate the desired paths points exactly. Simply calculating the length change terms in the structural error function, the adjustment amount for each path point is determined. A real-time controllable adjusting device is needed for the side link that accumulates structural error in the synthesis model. When the adjustable side-link is fixed at its length at first position for each phase, the mechanism can go back to the optimal multi-phase path generation mode.

#### 4.4 Optimal Multiple Path Generation: Adjustable Driving Dyad

Although the driving side fixed pivot and link length are not suitable for adjustment, its moving pivot remains adjustable. Adjusting the moving pivot  $B$  is equivalent to adjusting the length  $R_3$  and  $R_5$  at the same time.

With a few changes, the synthesis method in Section 4.3 is found to be capable to treat the driving dyad adjustment. For the driving dyad,  $R_5$  in Eq. (4.1) and (4.2) are adjustable. Suppose  $R_2 < R_5$ , and  $R_3$  and  $R_5$  has an increment of  $\Delta R$  in phase 2, then

$$R_2 + R_5 + \Delta R = R_{\max}^2 \quad (4.9)$$

$$R_5 - R_2 + \Delta R = R_{\min}^2 \quad (4.10)$$

Therefore,

$$R_{\max}^1 + \Delta R = R_{\max}^2 \quad (4.11)$$

$$R_{\min}^1 + \Delta R = R_{\min}^2 \quad (4.12)$$

The objective function to be minimized to find the circle point  $A$  is then

$$E_A = \{ [ (x_A - x_i^2)^2 + (y_A - y_i^2)^2 ]_{\max}^{1/2} - [ (x_A - x_i^1)^2 + (y_A - y_i^1)^2 ]_{\max}^{1/2} + [ (x_A - x_i^1)^2 + (y_A - y_i^1)^2 ]_{\min}^{1/2} - [ (x_A - x_i^2)^2 + (y_A - y_i^2)^2 ]_{\min}^{1/2} \}^2 \quad (4.13)$$

If  $R_2 > R_5$ , inverse the sign of  $\Delta R$  in Eq. (4.12), a similar  $E_A$  with different arrangement of terms can be obtained. Minimize  $E_A$  will find the best center point  $A$ .  $R_2$  and  $R_5$  are then obtained. The same constraints are to be imposed as in Section 4.3.1.

Once the driving dyad is obtained, the same procedure can be implemented as in Section 4.3.2 and 4.3.3 to synthesize the driven dyad as an optimal motion generation problem, either adjustable or non-adjustable.

The problem can also be solved as a multi-phase optimal motion generation problem with unknown coupler angles. The two dyads will then be composed into a single structural error and optimized at the same time. However, this method uses more unknowns including the unknown coupler angles, which is more difficult to optimize.

#### 4.5 Synthesis Example

A numerical example is solved in order to illustrate the method. In this example, only the driven-side fixed pivot is made adjustable. The paths to be synthesized are an ellipse and a pear-shaped curve. Each curve is specified by 20 points, as listed in Table 4.1. The curves are plotted in Figure 4.4.

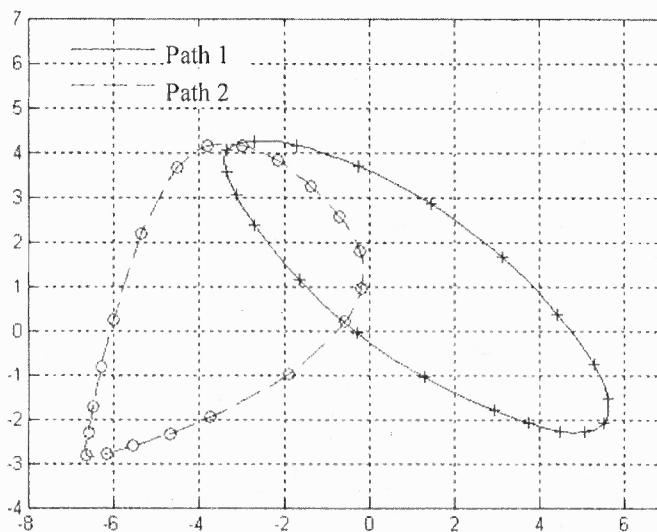


**Figure 4.4** Desired paths.

**Table 4.1** Desired Path Points

Point No.	Path 1		Path 2	
	<i>x</i>	<i>y</i>	<i>x</i>	<i>y</i>
1	-2.756	2.361	-5.365	2.170
2	-1.655	1.141	-5.994	0.258
3	-0.293	-0.060	-6.289	-0.833
4	1.279	-1.052	-6.484	-1.711
5	2.944	-1.804	-6.596	-2.309
6	3.747	-2.082	-6.633	-2.818
7	4.483	-2.264	-6.171	-2.790
8	5.073	-2.276	-5.545	-2.611
9	5.527	-2.072	-4.672	-2.325
10	5.607	-1.546	-3.732	-1.955
11	5.284	-0.765	-1.898	-0.976
12	4.430	0.372	-0.588	0.202
13	3.119	1.655	-0.202	0.956
14	1.447	2.848	-0.213	1.788
15	-0.272	3.703	-0.718	2.577
16	-2.706	4.245	-2.168	3.812
17	-3.349	4.062	-2.998	4.142
18	-3.355	3.555	-3.803	4.132
19	-3.154	3.003	-4.502	3.649
20	-2.756	2.361	-5.365	2.170

The proposed procedure is programmed on in Matlab® R2006a. Spline interpolation refines the paths to 100 points each. Given an initial guess (-2,-8), the first optimization finds the best center point  $A$  (0.225,-18.225), and  $R_{\max} = 22.583$ ,  $R_{\min} = 16.579$ . Joint  $A$  lies outside of both path loops, thus  $R_2 < R_5$ .  $R_2$  and  $R_5$  are then calculated:  $R_2 = 3.002$ ,  $R_5 = 19.581$ .

With an initial guess  $C_1(-5, -5)$ ,  $D^1(-10,-10)$ , and  $D^2(-15,-15)$ , the second optimization finds the other dyad at its first position of both phases:  $C_1^1(-0.275,-6.922)$ ,  $D^1(-8.679,-13.206)$ ,  $C_1^2(-1.823, -6.820)$ ,  $D^2(-12.19,-8.362)$ .

The optimized four-bar linkage is:  $R_2=3.002$ ,  $R_3=9.904$ ,  $R_4=10.500$ ,  $R_5=19.581$ ,  $R_6=9.679$ ,  $A(0.225,-18.225)$ ,  $D^1(-8.679,-13.206)$ , and  $D^2(-12.19,-8.362)$ .

Coordinates of all joints in their first position of each phase are constrained in the range  $[-20, 20]$  and the transmission angle is restricted between  $45^\circ$  and  $135^\circ$ . The joint coordinates of synthesized adjustable linkage in its first position of each phase are listed in Table 4.2. Fig. 4.5 shows the designed mechanism with the desired and generated paths. The desired paths are outlined by crosses or circles which present the specified points and the generated paths are plotted in solid or dashed line. The generated paths match the desired ones unexpectedly well, indicating that the example problem happens to have a high quality solution. The total work time is about 14 seconds on a Pentium 4 PC. This numerical example demonstrates the effectiveness of the proposed method.

**Table 4.2** Joint Positions of the Synthesized Adjustable Linkage

Joint	Phase 1		Phase 2	
	$x$	$y$	$x$	$y$
$A$	0.225	-18.225	0.225	-18.225
$B$	2.600	-16.389	2.138	15.907
$C$	-0.275	-6.911	-1.823	-6.820
$D$	-8.679	-13.206	-12.19	-8.362
$P$	-2.756	2.361	-5.365	2.170



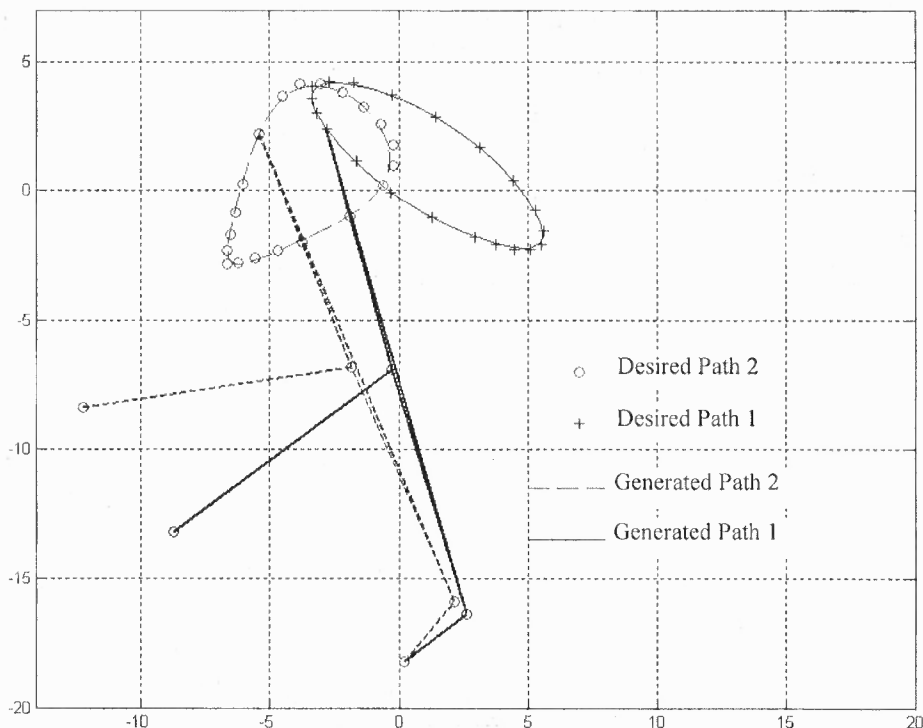


**Figure 4.5** Synthesized linkage and the generated and desired paths.

#### 4.6 Conclusion

An optimal synthesis method is developed for planar four-bar linkages adjustable for multi-phase continuous path generation. If only the driven dyad is adjustable, the non-adjustable driving dyad is first determined optimally using the full rotation requirement for both phases and the coupler angles at all design points are then calculated. The synthesis of the adjustable driven dyad is treated as a multi-phase optimal motion generation problem. The optimal motion synthesis method based on link length structural error, as developed in Chapter 3, is implemented to find the adjustable driven dyad. If the driving dyad is made adjustable, the method developed in Section 2.2 for optimal path generation can be used to find both dyads at the same time, or the method used to synthesize the non-adjustable driving dyad is slightly modified to represent the adjustment.

The link length structural error is a powerful alternative of conventional structural error which greatly simplifies the error function and facilitates the optimization process. A numerical example verifies the effectiveness of the proposed method. This synthesis method is very efficient in designing adjustable linkages capable of tracing a number of target points in each phase with an acceptable error. The adjustable path generation mechanism synthesized with this method can also be made continuously adjustable to achieve precision path points in both phases.

## CHAPTER 5

### OPTIMAL MULTI-PHASE FUNCTION GENERATION

#### 5.1 Optimal Function Generation

The classical function generation method uses Chebyshev spacing to pick precision points in the variable range of the function to be synthesized and then solves loop equations for the linkage parameters. A four-bar linkage synthesized with this method can precisely generate a given function at up to five points.

To match the function at more points, some error, also called structural error, has to be allowed between the generated and the desired functions, which leads to the optimal synthesis of function generation mechanisms. The optimal synthesis technique is designed to synthesize mechanisms that approximate given functions at more points with less overall structural error (notice that for precision point function synthesis, error still exists between the selected design points).

The conventional way of constructing the structural error for function generation directly compares the generated output angles with the desired ones at all prescribed input positions.

In Figure 5.1, the origin of the coordinate system  $XOY$  is located at joint  $A$  and its  $x$  axis at the direction of  $AD$  and the link length  $AD$  is set to  $R_1=1$ . These settings eliminate the scaling and rotating of the linkage, which will result in linkages that are considered the same as the original one. For the design of a four-bar function generation linkage, the function to be generated,  $y=f(x)$ , is mapped to the input and output link angles  $\theta_{2di}$  and  $\theta_{4di}$ . According to its definition, the structural error can be given as

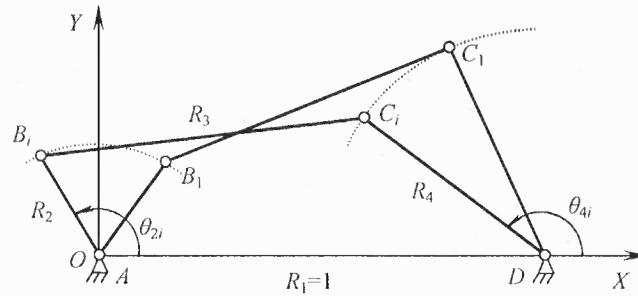


**Figure 5.1** A four-bar function generator.

$$E_R = \sum_{i=1}^n \eta_i (\theta_{4gi} - \theta_{4di})^2 \quad (5.1)$$

$\theta_{4gi}$  are the actual output link angles of the generated linkage at desired input angles  $\theta_{2di}$ .

$\theta_{4gi}$  can be obtained from Freudenstein's equation [1],

$$K_1 \cos \theta_2 + K_2 \cos \theta_4 + K_3 = -\cos(\theta_2 - \theta_4) \quad (5.2)$$

where

$$K_1 = \frac{R_1}{R_4}, K_2 = \frac{-R_1}{R_2}, K_3 = \frac{R_3^2 - R_1^2 - R_2^2 - R_4^2}{2R_2R_4} \quad (5.3)$$

It can be expected that the solution of  $\theta_{4gi}$  from Eq. (5.2) does not appear simple, which makes the optimization less efficient. In the next section a new method of optimally synthesizing function generation mechanisms base on coupler link length structural error is to be developed.

## 5.2 Optimal Function Generation Based on Coupler Link Length Structural Error

The idea of link length structural error has worked well for optimal motion and path generation. This section explores its capability in approximate function generation.

### 5.2.1 Linear Spacing

*Chebyshev's spacing* is usually used to minimize the structural error of the linkage at points other than the chosen precision points in function generation. This technique, based on *Chebyshev Polynomials*, is often used as a first guess. Although it works for a few precision points, it is not applicable for optimal function generation in which a number of approximate points are needed, because the resulted Chebyshev polynomials are of too high order.

Since there are many points chosen in the range of the function's independent variable for optimal function generation, the spacing becomes less important. To simplify the synthesis, *linear spacing* is used instead. With linear spacing, the check points are evenly chosen between the boundaries of the range.

Suppose the function to be generated is

$$y = f(x), x \in (x_a, x_b), y \in (y_a, y_b) \quad (5.4)$$

Totally  $n$  points are evenly chosen from the range  $(x_a, x_b)$ . The resulted  $x_i$  and corresponding  $y_i$  are

$$(x_i, y_i) = \left(x_a + \frac{x_b - x_a}{n-1}, f(x_i)\right), i = 1, 2, \dots, n \quad (5.5)$$

$(x_i, y_i)$  is to be mapped to  $(\theta_{2di}, \theta_{4di})$ , the desired input and output angles for a four-bar linkage. The relationship between the changes of  $x$  and  $\theta_{2d}$  is again linear. Suppose the input angle is to be in the range  $(\theta_{2a}, \theta_{2b})$ , and the output in the range  $(\theta_{4a}, \theta_{4b})$ , then

$$(\theta_{2di}, \theta_{4di}) = \left(\theta_{2a} + \frac{\theta_{2b} - \theta_{2a}}{x_b - x_a}(x_i - x_a), \theta_{4a} + \frac{\theta_{4b} - \theta_{4a}}{y_b - y_a}(y_i - y_a)\right) \quad (5.6)$$

$(\theta_{2a}, \theta_{2b})$  and  $(\theta_{4a}, \theta_{4b})$  can be either prescribed or design variables.

The linear spacing greatly simplifies the chosen of check points while does not obviously affect the accuracy of the resultant mechanism.

### 5.2.2 Coupler Link Length Structural Error

The length of the coupler link is chosen to be flexible, as in Fig. 5.2. When the input link AB and output link CD is forced to pass through their desired positions demanded by the given function, the link BC changes its length if the linkage can not generate the function precisely. The change of link length  $R_3$  reflects the error of the generated linkage. This length change can be measured as

$$E_R = \sum_{i=1}^n E_{Ri} = \sum_{i=2}^n [(B_i - C_i)(B_i - C_i)^T - (B_1 - C_1)(B_1 - C_1)^T]^2 \quad (5.7)$$

$$\begin{aligned}
 B_i &= (x_{B_i}, y_{B_i})^T = (R_2 \cos \theta_{2di}, R_2 \sin \theta_{2di})^T \\
 C_i &= (x_{C_i}, y_{C_i})^T = (R_1 + R_4 \cos \theta_{4di}, R_4 \sin \theta_{4di})^T
 \end{aligned}
 \tag{5.8}$$

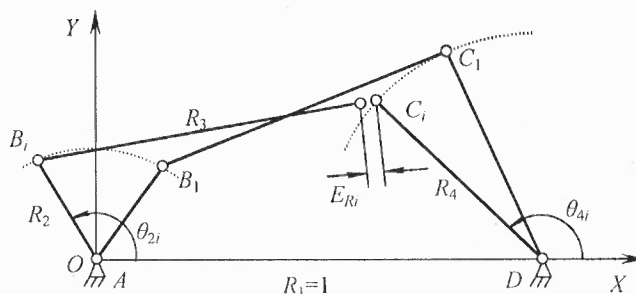


**Figure 5.2** The coupler link length structural error.

The smaller  $E_R$ , the less are the changes the link BC needs to make during the movement of link AB and CD through the desired angles pairs  $(\theta_{2di}, \theta_{4di})$ . When  $E_R$  is zero, the designed linkage is able to generate the desired function at all chosen points. Hence  $E_R$  effectively represents the overall error of the synthesized linkage and makes a satisfying structural error.

Notice that the coupler link length structural error in Eq. (5.7) is a pure forth order polynomial of only two design variables  $(R_2, R_4)$  (suppose the input and output angle range  $(\theta_{2a}, \theta_{2b})$  and  $(\theta_{4a}, \theta_{4b})$  are prescribed, otherwise four additional variables apply), much simpler than the structural error derived directly from the conventional definition.

### 5.2.3 Validation

Similar as in Section 2.1.2, the coupler link length structural error can be proven to be equivalent to the conventional one which compares the generated and desired crank angles directly. That is to prove that when input crank is set to the desired angle, the output angle

error and the coupler link length error are infinitesimals of the same order.

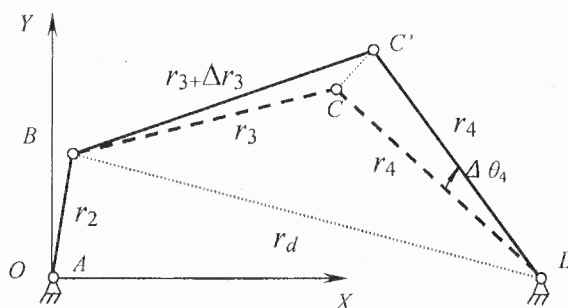


**Figure 5.3** A four-bar function generator with coupler link length error.

As shown in Figure 5.3, the input crank  $AB$  is fixed at the desired input angle. The error in length of link  $BC$ ,  $\Delta r_3$ , will move the joint  $C$  to a generated position  $C'$ . Because of the transmission constraint, link  $BC$  and  $CD$  are not collinear. For triangular  $\triangle BCD$ , the law of cosines gives

$$\cos \angle BDC = \frac{r_4^2 + r_d^2 - r_3^2}{2r_4r_d} \quad (5.9)$$

Give  $r_3$  a small change  $\Delta r_3$ ,

$$\cos \angle BDC' = \frac{r_4^2 + r_d^2 - (r_3 + \Delta r_3)^2}{2r_4r_d} = \cos \angle BDC - \frac{2r_3\Delta r_3 + \Delta r_3^2}{2r_4r_d} \quad (5.10)$$

$$\cos \angle BDC' - \cos \angle BDC = -\frac{2r_3\Delta r_3 + \Delta r_3^2}{2r_4r_d} \quad (5.11)$$



As has been proven previously,

$$\Delta\theta_4 = O(\cos \angle BDC' - \cos \angle BDC) = O(\Delta r_3 / r_d) \quad (5.12)$$

$\Delta\theta_4$  is a same order infinitesimal as  $\Delta r_3 / r_d$ . Therefore when the coupler link length structural error is small, the conventional structural error for function generation is believed to be small.

#### 5.2.4 Constraints

##### *a. Link Lengths*

The link length  $R_2$  and  $R_4$  may need to be constrained in a suitable range that is not too long or too short:

$$r_a < R_2 < r_b, r_a < R_4 < r_b \quad (5.13)$$

No Grashof's constraint is needed for the link lengths for the input link is not required to fully rotate.

##### *b. Transmission Angle*

Given coordinates of pivots  $B$ ,  $C$  and  $D$ , the transmission angle  $\mu$  ( $\angle BCD$ ) can be easily calculated. The transmission angle is limited to

$$\mu_{\min} < \mu < \mu_{\max} \quad (5.14)$$

No additional constraint has to be imposed to this optimization problem. The minimization can be implemented using Matlab. This optimal synthesis method provides an easy way to find the optimum linkage that approximate a given function at many points. Another advantage of this form of structural error is that it greatly facilitates the optimal synthesis of adjustable function generation mechanisms. The next section explores its potential in this field.

### **5.3 Multiple Approximate Function Generation**

Adjustable function generation mechanisms can generate multiple functions in different phases, thus have attracted attention of researchers. Reported synthesis methods for multiple function generation have focused on the synthesis of mechanisms that generates several precision function points. The designed adjustable mechanism can achieve even less precision points for each of desired functions than a nonadjustable mechanism can do for a single function. To achieve more design points for each phase, optimal synthesis method developed in Section 5.2 is introduced into the synthesis of adjustable function generator.

For a four-bar function generator, the two fixed pivot as the input and output axes are not recommended to be adjusted. The adjustment to the moving pivot is equivalent to the adjustment to the coupler link length. The side-link lengths are also adjustable.

Suppose the functions to be generated are

$$\begin{aligned} y_1 &= f_1(x), \\ y_2 &= f_2(x) \end{aligned} \quad (5.15)$$

where  $x_1 \in (x_{1a}, x_{1b})$ ,  $y_1 \in (y_{1a}, y_{1b})$ ,  $x_2 \in (x_{2a}, x_{2b})$ ,  $y_2 \in (y_{2a}, y_{2b})$ . The linear spacing is used again to choose  $n$  points from the range  $(x_{1a}, x_{1b})$  and  $(x_{2a}, x_{2b})$  and the corresponding  $y$  values are calculated. The chosen points are then mapped to the desired input and output angles for a four-bar linkage,  $(\theta_{2di}^1, \theta_{4di}^1)$  and  $(\theta_{2di}^2, \theta_{4di}^2)$ .

### 5.3.1 Adjustable Coupler Link Length

Since the coupler link has been already chosen to be the flexible link that carries the structural error, the adjustment to it can be easily modeled by adding another term for phase 2 to the structural error, as in Eq. (5.16). When the input link AB and output link CD is forced to pass through their desired positions demanded by the given function, the link BC changes its length if the linkage can not generate the function precisely. The change of link length  $R_3$  reflects the error of the generated linkage. This length change can be measured as

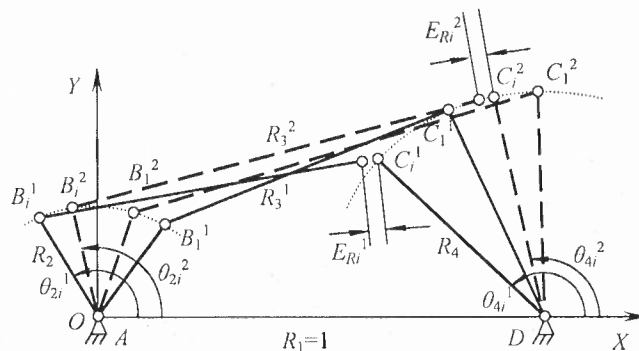


**Figure 5.4** The adjustable coupler link length four-bar function generator.

$$E_R = E_R^1 + E_R^2 = \sum_{i=2}^n \{ [(B_i^1 - C_i^1)(B_i^1 - C_i^1)^T - (B_1^1 - C_1^1)(B_1^1 - C_1^1)^T]^2 + [(B_i^2 - C_i^2)(B_i^2 - C_i^2)^T - (B_1^2 - C_1^2)(B_1^2 - C_1^2)^T]^2 \} \quad (5.16)$$

$$\begin{aligned} B_i^1 &= (x_{Bi}^1, y_{Bi}^1)^T = (R_2 \cos \theta_{2di}^1, R_2 \sin \theta_{2di}^1)^T, C_i^1 = (x_{Ci}^1, y_{Ci}^1)^T = (R_1 + R_4 \cos \theta_{4di}^1, R_4 \sin \theta_{4di}^1)^T \\ B_i^2 &= (x_{Bi}^2, y_{Bi}^2)^T = (R_2 \cos \theta_{2di}^2, R_2 \sin \theta_{2di}^2)^T, C_i^2 = (x_{Ci}^2, y_{Ci}^2)^T = (R_1 + R_4 \cos \theta_{4di}^2, R_4 \sin \theta_{4di}^2)^T \end{aligned} \quad (5.17)$$

The unknowns are again  $(R_2, R_4)$  (plus the input and output angle range  $(\theta_{2a}^1, \theta_{2b}^1)$ ,  $(\theta_{2a}^2, \theta_{2b}^2)$ ,  $(\theta_{4a}^1, \theta_{4b}^1)$  and  $(\theta_{4a}^2, \theta_{4b}^2)$  if they are not prescribed).

### 5.3.2 Adjustable Side Link Length

Suppose the length of the side link  $CD$  is adjustable,  $R_4$  now has two values for the two phases,  $R_4^1$  and  $R_4^2$ , respectively. Similar to adjustable coupler link length problem, the overall structural error is

$$E_R = E_R^1 + E_R^2 = \sum_{i=2}^n [(B_i^1 - C_i^1)(B_i^1 - C_i^1)^T - (B_1^1 - C_1^1)(B_1^1 - C_1^1)^T]^2 + \sum_{i=1}^n [(B_i^2 - C_i^2)(B_i^2 - C_i^2)^T - (B_1^1 - C_1^1)(B_1^1 - C_1^1)^T]^2 \quad (5.18)$$

$$\begin{aligned} B_i^1 &= (x_{Bi}^1, y_{Bi}^1)^T = (R_2 \cos \theta_{2di}^1, R_2 \sin \theta_{2di}^1)^T, C_i^1 = (x_{Ci}^1, y_{Ci}^1)^T = (R_1 + R_4^1 \cos \theta_{4di}^1, R_4^1 \sin \theta_{4di}^1)^T \\ B_i^2 &= (x_{Bi}^2, y_{Bi}^2)^T = (R_2 \cos \theta_{2di}^2, R_2 \sin \theta_{2di}^2)^T, C_i^2 = (x_{Ci}^2, y_{Ci}^2)^T = (R_1 + R_4^2 \cos \theta_{4di}^2, R_4^2 \sin \theta_{4di}^2)^T \end{aligned} \quad (5.19)$$

The adjusting device can be made real-time controllable so that the coupler link can follow the correct length required by the desired functions. The linkage then can generate the functions precisely at all selected design points.

### 5.4 Numerical Example

A numerical example is solved to verify the effectiveness of the proposed method. In this example, the coupler link length is adjustable. The two functions to be generated are:

1. Phase 1:  $y_1 = \sin x$ ,  $0 \leq x \leq 90^\circ$  and  $90^\circ \leq \theta \leq 210^\circ$ ,  $60^\circ \leq \phi \leq 120^\circ$ ;
2. Phase 2:  $y_2 = x^{1.5}$ ,  $0 \leq x \leq 1$  and  $25^\circ \leq \theta \leq 95^\circ$ ,  $70^\circ \leq \phi \leq 105^\circ$

20 checking points are evenly chosen over each independent variable range. The desired input and output angles are listed in Table 5.1. The ground link length  $R_1$  is set to 1 and other link lengths are limited between 0.1 and 10. The transmission angle is set as  $45^\circ \leq \mu \leq 135^\circ$ .

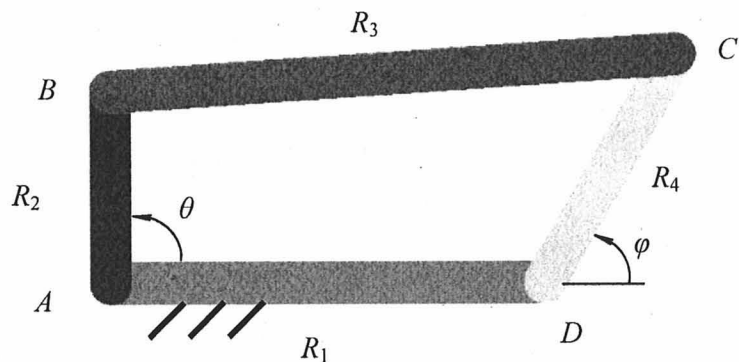
Given an initial guess of  $R_2 = R_4 = 0.5$ , the optimization finds the solution for  $R_2$  and  $R_4$ .  $R_3$  and  $R_3'$  are obtained from the distance between joints **B** and **C** at their first position of each phase. The optimized adjustable four-bar linkage is given in Table 5.2. Figure 5.5 shows the two phases of the adjustable linkage. The two phases share the same geometry except a different coupler link length. Also notice that the starting input angles are different according to the different desired functions. The desired and generated functions are plotted in Figure 5.6.

**Table 5.1** Desired Input and Output Angles

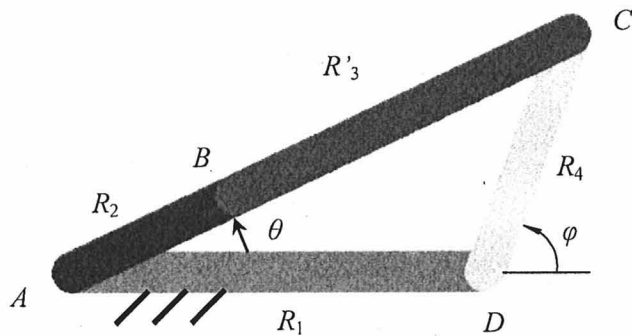
Point No.	Phase 1		Phase 2	
	$\theta$	$\varphi$	$\theta$	$\varphi$
1	90.0000	60.0000	25.0000	70.0000
2	96.3158	64.9548	28.6842	70.4226
3	102.6316	69.8757	32.3684	71.1953
4	108.9474	74.7291	36.0526	72.1959
5	115.2632	79.4820	39.7368	73.3809
6	121.5789	84.1017	43.4211	74.7249
7	127.8947	88.5568	47.1053	76.2110
8	134.2105	92.8169	50.7895	77.8268
9	140.5263	96.8528	54.4737	79.5625
10	146.8421	100.6369	58.1579	81.4104
11	153.1579	104.1434	61.8421	83.3640
12	159.4737	107.3484	65.5263	85.4180
13	165.7895	110.2300	69.2105	87.5675
14	172.1053	112.7684	72.8947	89.8085
15	178.4211	114.9464	76.5789	92.1376
16	184.7368	116.7490	80.2632	94.5513
17	191.0526	118.1640	83.9474	97.0469
18	197.3684	119.1817	87.6316	99.6218
19	203.6842	119.7951	91.3158	102.2735
20	210.0000	120.0000	95.0000	105.0000

**Table 5.2** Optimized Adjustable Function Generating Linkage

$R_1$	$R_2$	$R_3$	$R_4$	$R_3'$
1	0.4390	1.3043	0.6032	0.8942

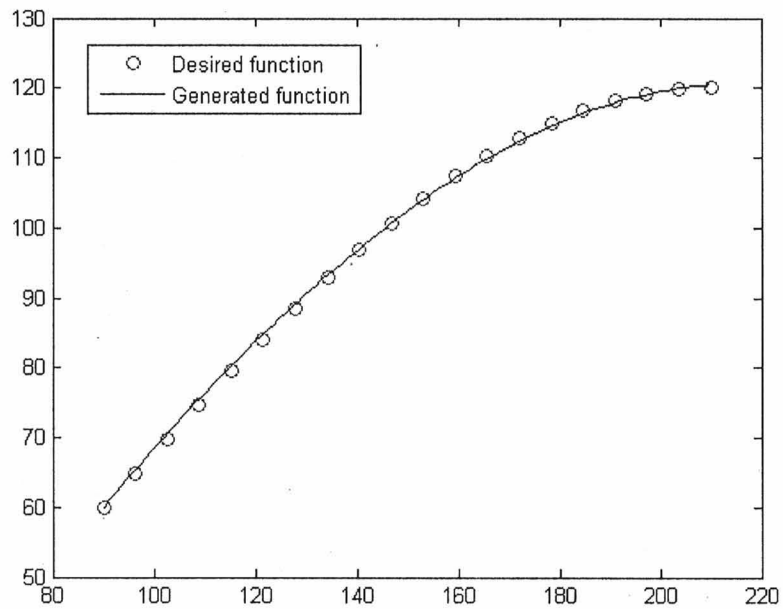


(a) Phase 1:  $R_1=1$ ,  $R_2=0.4390$ ,  $R_3=1.3043$ ,  $R_4=0.6032$

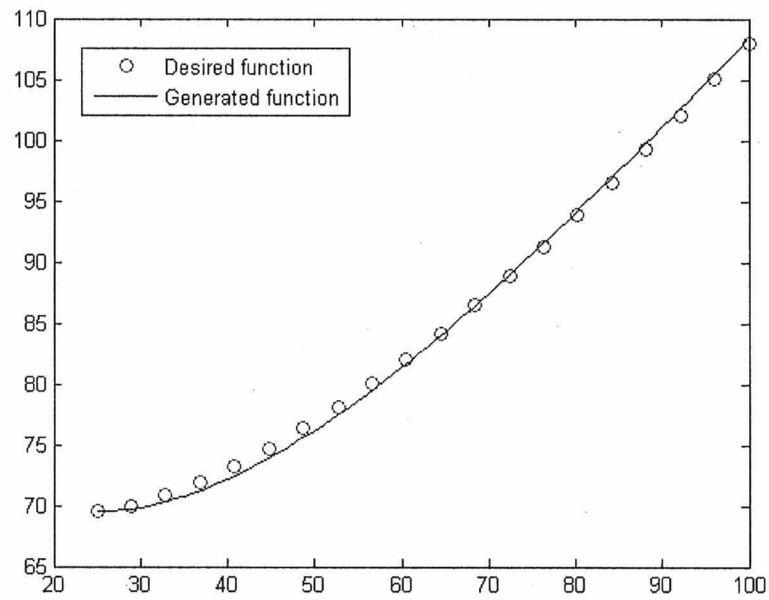


(b) Phase 2:  $R_1=1$ ,  $R_2=0.4390$ ,  $R_3=0.8942$ ,  $R_4=0.6032$

**Figure 5.5** The optimized adjustable function generator: (a) phase 1; (b) phase 2.



(a)



(b)

**Figure 5.6** The desired and generated functions: (a)  $y = \sin x$ ; (b)  $y = x^{1.5}$ .



## 5.5 Conclusion

The idea of link length structural error was applied to the optimal synthesis of adjustable function generation mechanisms successfully. The coupler link length fluctuation was chosen to be the structural error because it matches the function generation problem perfectly. This arrangement led to a structural error that was not only concise but also effective. The method considerably simplified the modeling of optimal function generation problem and facilitates the optimization process and handled the adjustment to the coupler link or side link length easily. It was also capable of generate many precise points with the assistance of a continuously adjustable link length. Numerical synthesis examples have not been solved to demonstrate the effectiveness of this method.

## CHAPTER 6

### CONCLUSION

Adjustable mechanisms provide degrees of flexibility while retaining desirable features of one degree of freedom close-loop mechanisms, such as simplicity, stability, and high speed, load, and precision capabilities. However, previous studies on adjustable mechanisms have focused on synthesis of mechanisms generating multi-set of exact positions. By exact synthesis, an adjustment to the mechanism can add only one or two additional design positions to the mechanism, and the positions are divided into several phases. Therefore each phase contains only a few positions, which is insufficient and not cost-effective.

Various optimal synthesis techniques have been developed to achieve more design positions. However, no work is reported to apply optimal synthesis methods to adjustable mechanisms except a method developed by Zhou and Ting [39], which is limited to generate multiple tangential continuous curves.

This research is believed to be the first to develop a general optimal synthesis method for adjustable planar mechanisms generating multi-phase approximate motions, continuous paths, and functions. In this dissertation, the optimal synthesis method based on link length structural error is developed, validated, and extended to the optimal synthesis of adjustable mechanisms for three typical synthesis tasks.

For motion generation, the synthesis model of an adjustable optimal dyad is established for three types of adjustments (the adjustment to the moving pivot, fixed pivot, and the link length) and their combinations. An adjustable four-bar linkage is optimized based on the dyad model under proper constraints including the link length requirements,

the Grashof's condition, and the transmission angle requirement.

For multiple continuous path generation, the driving dyad is synthesized first by an optimization using the full rotation requirement. The coupler angles are then obtained and the synthesis of the driven adjustable dyad becomes an optimal multi-phase motion generation problem, which had been solved.

For optimal multi-phase function generation, the coupler length structural error fits the nature of the problem, making a very simple form of structural error. The suitable adjustments to the function generation four-bar linkage are made to the lengths of the coupler link or the side links.

The use of link length structural error significantly simplified the optimal synthesis of adjustable mechanisms and enhances the efficiency of the optimization. The presented optimal synthesis method is found to have a remarkable advantage: with continuously adjustable link lengths, the linkage synthesized under this method can generate the desired motion exactly. The link length structural error aims directly at the required link length changes so that the required link length changes are already available once the linkage is optimized. The synthesized mechanism can work in two different "modes": "precision mode" in which the relevant link lengths are adjusted real-time at the calculated amount, or "optimum mode" in which the link lengths are fixed at their optimal length for each phase while the linkage generates the desired multi-phase motions approximately.

Suggested future studies include: (1) to extend the link length structural error based optimal synthesis method to planar five-bar and multi-loop mechanisms, and then spatial mechanisms; (2) to clearly identify what types of motions, paths, or functions are in nature suitable to be generated by the proposed method and what are not; (3) to build a software

package or data base, from which engineers can find linkage solutions from desired motion;

(4) to examine the influence of unexpected linkage dimension changes (from sources such as component dimension error, dynamic loads and responses, thermal deformation, and link flexibility) on the accuracy of generated motions.

## REFERENCES

- [1] G. N. Sandor, A. G. Erdman, *Advanced Mechanism Design: Analysis and Synthesis*, Vol. 2, Prentice-Hall, 1984.
- [2] R. D. Bonnell, Graphical Synthesis of an adjustable four-bar linkage, *Design News*, March 18, 1964.
- [3] A. Ahmad, K. J. Waldron, Synthesis of adjustable planar four-bar mechanisms, *Mechanism and Machine Theory* 14 (3) (1979) 405-411.
- [4] A. Ahmad, Synthesis of adjustable planar four-bar mechanisms, Ph.D. Dissertation, University of Houston, USA, 1979.
- [5] H. Funabashi, N. Iwatsuki, Y. Yoshiaki, A synthesis of crank length adjusting mechanisms, *Bulletin of JSME* 29 (252) (1986) 1946-1951.
- [6] A. J. Wilhelm, Kinematic synthesis of adjustable linkages for motion generation, Ph.D. Dissertation, The Wichita State University, USA, 1989.
- [7] T. Chuenchom, S. Kota, Synthesis of programmable mechanisms using adjustable dyads, *ASME Journal of Mechanical Design* 119 (2) (1997) 232-237.
- [8] T. Chuenchom, Kinematic synthesis of adjustable robotic mechanisms, Ph.D. Thesis, The University of Michigan, USA, 1993.
- [9] S. J. Wang, R. S. Sodhi, Kinematic synthesis of adjustable moving pivot four-bar mechanisms for multi-phase motion generation, *Mechanism and Machine Theory* 31 (4) (1996) 459-474.
- [10] S. J. Wang, Kinematic Synthesis of adjustable four-bar mechanisms for multi-phase motion generation, Ph.D. Dissertation, New Jersey Institute of Technology, USA, 1993.
- [11] B. Hong, A. G. Erdman, A method for adjustable planar and spherical four-bar linkage synthesis, *ASME Journal of Mechanical Design* 127 (2005) 456-463.
- [12] K. Russell, R. S. Sodhi, Kinematic synthesis of planar five-bar mechanisms for multi-phase motion generation, *JSME International Journal, Series C*, 47 (2004) 345-349.
- [13] K. Russell, R. S. Sodhi, Kinematic synthesis of adjustable RRSS mechanisms for multi-phase motion generation, *Mechanism and Machine Theory* 36 (2001) 939-952.

- [14] K. Russell, R. S. Sodhi, Kinematic synthesis of adjustable RRSS mechanisms for multi-phase motion generation with tolerances, *Mechanism and Machine Theory* 37 (2002) 279-294.
- [15] K. Russell, R. S. Sodhi, Kinematic synthesis of adjustable RSSR-SS mechanisms for multi-phase finite and multiply separated positions, *ASME Journal of Mechanical Design* 125 (2003) 847-853.
- [16] D. C. Tao, S. Krishnamoorthy, Linkage mechanism adjustable for variable coupler curves with cusps, *Mechanism and Machine Theory* 13 (6) (1978) 577-583.
- [17] D. C. Tao, S. Krishnamoorthy, Linkage mechanism adjustable for variable symmetrical coupler curves with a double point, *Mechanism and Machine Theory* 13 (6) (1978) 585-591.
- [18] J. F. McGovern, G. N. Sandor, Kinematic synthesis of adjustable mechanisms (Part 1: function generation), *ASME Journal of Engineering for Industry* 95 (2) (1973) 417-422.
- [19] J. F. McGovern, G. N. Sandor, Kinematic synthesis of adjustable mechanisms (Part 2: path generation), *ASME Journal of Engineering for Industry* 95 (2) (1973) 423-429.
- [20] L. Huston, S. Kramer, Complex number synthesis of four-bar path generating mechanisms adjustable for multiple tangential circular arcs, *ASME Journal Mechanical Design* 104 (1982) 185-191.
- [21] H. Shimojima, K. Ogawa, A. Fujiwara, O. Sato, Kinematic synthesis of adjustable mechanisms, *Bulletin of JSME* 26 (214) (1983) 627-632.
- [22] K. Russell, R. S. Sodhi, On the design of slider-crank mechanisms. Part II: multi-phase path and function generation *Mechanism and Machine Theory* 40 (2005) 301-317.
- [23] C. F. Chang, Synthesis of adjustable four-bar mechanisms generating circular arcs with specified tangential velocities, *Mechanism and Machine Theory* 36 (3) (2001) 387-395.
- [24] A. Ahmad, K. J. Waldron, Design techniques for adjustable function generators, *Proceedings - OSU Applied Mechanisms Conference (Oklahoma State University)* 1979.
- [25] D. P. Naik, C. Amarnath, Synthesis of adjustable four bar function generators through five bar loop closure equations, *Mechanism and Machine Theory* 24 (6) (1989) 523-526.

- [26] T. S. Mruthyunjaya, M. R. Raghavan, Derivative synthesis of adjustable four-bar mechanisms for function generation, American Society of Mechanical Engineers Issue 76 (1976).
- [27] K. Russell, W. Lee, R. S. Sodhi, On least squares based motion generation of adjustable five bar spherical mechanisms, 12<sup>th</sup> IFToMM World Congress, Besancon (France), June 18-21, 2007.
- [28] D. A. Hoeltzel, W. H. Chieng, Pattern matching synthesis as an automated approach to mechanism design, ASME Journal of Mechanical Design 112 (2) (1990) 190-199.
- [29] K. Watanabe, Application of natural equations to the synthesis of curve generating mechanisms, Mechanism and Machine Theory 27 (3) (1992) 261-273.
- [30] H. J. Kim, R. S. Sodhi, Synthesis of planar four-bar mechanisms for generating a prescribed coupler curve with five precision points, Journal of Applied Mechanisms and Robotics 3 (2) (1996) 9-13.
- [31] J. Mariappan, S. Krishnamurty, A Generalized exact gradient method for mechanism synthesis, Mechanism and Machine Theory 31 (4) (1996) 413-421.
- [32] R. Sancibrian, F. Viadero, P. Garcia, A. Fernandez, Gradient-based optimization of path synthesis problems in planar mechanisms, Mechanism and Machine Theory 39 (2004) 839-856.
- [33] J. A. Cabrera, A. Simon, M. Prado, Optimal synthesis of mechanisms with genetic algorithms, Mechanism and Machine Theory 37 (2002) 1165-1177.
- [34] A. Smaili, N. Diab, Optimum synthesis of hybrid-task mechanisms using ant-gradient search method, Mechanism and Machine Theory 42 (2007) 115-130.
- [35] M. A. Laribi, A. Mlika, L. Romdhane, S. Zegloul, A combined genetic algorithm-fuzzy logic method (GA-FL) in mechanisms synthesis, Mechanism and Machine Theory 39 (2004) 717-735.
- [36] A. Vasiliu, B. Yannou, Dimensional synthesis of planar mechanisms using neural networks: application to path generator linkages, Mechanism and Machine Theory 36 (2001) 299-310.
- [37] J. Vallejo, R. Aviles, A. Hernandez, E. Amezua, Nonlinear optimization of planar linkages for kinematic synthesis, Mechanism and Machine Theory 30 (4) (1995) 501-518.

- [38] H. Zhou, E. H. M. Cheung, Optimal synthesis of crank-rocker linkages for path generation using the orientation structural error of the fixed link, *Mechanism and Machine Theory* 36 (2001) 973-982.
- [39] H. Zhou, K. L. Ting, Adjustable slider-crank linkages for multiple path generation, *Mechanism and Machine Theory* 37 (2002) 499-509.
- [40] A. G. Erdman, *Modern Kinematics: Developments in the Last Forty Years*, Wiley-Interscience Publication, 1993.
- [41] A. A. Smaili, N. A. Diab, N. A. Atallah, Optimum synthesis of mechanisms using tabu-gradient search algorithm, *Journal of Mechanical Design* 127 (2005) 917.
- [42] R. Akhras, J. Angeles, Unconstrained nonlinear least-square optimization of planar linkages for rigid-body guidance, *Mechanism and Machine Theory* 25 (1990) 97-118.
- [43] J. Angeles, A. Alivizatoss, R. Akhras, An unconstrained nonlinear least-square method of optimization of RRRR planar path generators, *Mechanism and Machine Theory* 23 (1988) 343-353.
- [44] M. D. Lioa, V. Cossalter, R. Lot, On the use of natural coordinates in optimal synthesis of mechanisms, *Mechanism and Machine Theory* 35 (2000) 1367-1389.
- [45] I. Ullah, S. Kota, Optimal synthesis of mechanisms for path generation using Fourier Descriptors and global search methods, *Journal of Mechanical Design* 119 (1997) 504-511.